A VELOCITY TRANSFER FUNCTION ANALYSIS OF FORCED CONVECTION HEAT TRANSFER

by

MICHAEL KENT MAHAFFEY

B. S., Kansas State University, 1964

A MASTER'S THESIS

submitted in partial fulfillment of the

requirements for the degree

MASTER OF SCIENCE

Department of Nuclear Engineering

KANSAS STATE UNIVERSITY
Manhattan, Kansas

1966

Approved by:

John O. Mingle
Major Professor

TABLE OF CONTENTS

LIST OF TABLES

LIST OF FIGURES

NOMENCLATURE

A	Area (ft^2)
C	Constants of integration
C_p	Heat capacity ($BTU/^oF\text{-}lb_m$)
dv	Differential volume (ft^3)
dz	Differential length (ft)
e	Internal energy (BTU/lb_m)
E	Ratio of Bessel functions
f_1	Function of s and r
$\bar{f}$	Laplace transform of $f(\tau)$
g_o	Function of s and r
g_1	Function of s and r
h	Heat transfer coefficient ($BTU/hr\text{-}ft\text{-}^oF$)
H	Enthalpy (BTU/lb_m)
I_o	Modified Bessel function of zero order, first kind
I_1	Modified Bessel function of first order, first kind
K_1	Modified Bessel function of first order, second kind
K_o	Modified Bessel function of zero order, second kind
k	Thermal conductivity ($BTU/hr\text{-}ft\text{-}^oF$)
L	Total length of the tube (ft)
m	Mass (lb)
p	Pressure (lb/ft^2)
P_x	Work (ft-lb)
q	Heat flow (BTU/hr)
q''	Heat flux ($BTU/hr\text{-}ft^2$)

q'''	Heat generation (BTU/hr-ft^2)
r, r_i, r_o	Characteristic radii of the tube (ft)
s	Laplace transform variable (sec)$^{-1}$
t	Wall temperature (^oF)
t'	Perturbed wall temperature (^oF)
u	Velocity of the coolant (ft/hr)
u_o	Initial velocity (ft/hr)
v	Specific volume (ft^3)
V	Volume (ft^3)
W	Constants of the exponential series
z	Distance along the tube (ft)
α	Thermal diffusivity (ft^2/hr)
ε	Order of perturbation
θ	Coolant temperature (^oF)
μ	Variable relating to r, $r\sqrt{s/\alpha}$
ρ	Density (lb/ft^3)
τ	Time (hr)
ω_j	Roots of the approximate transform function (sec^{-1})

1.0 INTRODUCTION

The problems involved in transferring the heat produced in a nuclear reactor core are many and varied. One which is of great concern is the behavior of single fuel elements due to abrupt changes in coolant velocity. If this behavior can be predicted and extended to the entire reactor core, then experiments can be limited to a single fuel element instead of a complete reactor core resulting in substantial reductions in cost and time.

In this study digital computer methods are used in conjunction with a perturbation technique to predict the response to changes in coolant velocity of a stainless steel test section contained in a pressurized water heat transfer loop. The transfer function of outlet temperature - coolant velocity will be formulated and utilized in predicting temperature response to step changes in velocity. Selected results will be compared with experimental data gathered from the heat transfer loop operated by the Nuclear Engineering Department of Kansas State University.

2.0 PREVIOUS INVESTIGATIONS

Investigations in heat transfer today center around both transient and steady state research in almost all temperature ranges in which energy transport is practical. Turbulent flow with forced convection has long held the interest of many engineers due to its very nature of thorough mixing and good heat transfer properties. This very mixing action, statistical in nature, has led to empirical attempts to describe and predict experimental results (6) rather than a purely theoretical solution. Such attempts have consisted of obtaining data from heat transfer loops and similar apparatus, and attempting to correlate empirically the coefficient of heat transfer and other important parameters such as burnout or critical heat flux.

The subject of excursions in power and temperature has been dealt with theoretically in many references (16,17,15,7,10) but only in the latter has a transfer function for velocity been proposed. Both exact theoretical and approximate numerical techniques have been propounded to predict the changes in the parameters of coolant outlet temperature and inner wall temperature. The exact theoretical solutions are complicated and somewhat time-consuming when compared with other numerical approaches.

A theoretical solution to the problem of forced flow in a heated tube has been proposed by Arpaci and Clark (1) in a series of papers dealing with the response of the heat transfer surface temperature and fluid-surface temperature difference to power transients. They propose the description of the above parameters in space and time as a combination of dimensionless, mathematical functions in graphical form. The papers are accompanied by

data which appears to corroborate their solutions.

Many approximate solutions were proposed in the late 1950's by Takahashi (16,17), Dusinberre (7), and Rizika (15). Work of a more recent nature has been done for two models representing reactor systems by Gyftopoulos and Smets (10). They derive transfer functions for slab geometries from the basic equations of heat transfer using Laplace transform technique. The velocity - outlet temperature transfer function is solved for by a perturbation approach.

Some recent investigation in analog and theoretical models has been done at Oak Ridge National Laboratory by Ball (2,3). The latest article describes the use of dimensionless frequency response diagrams to determine accuracies of lumped parameter approximations of heat transfer systems. Dimensionless system parameters make it possible to use general purpose plots to find the error in approximations as a function of the frequency of perturbation. The earlier article deals more specifically with plug flow systems and analog models which can be used to simulate their behavior. One special case which he treats is that of the insulated, heated pipe with central coolant flow. These conditions apply also to the loop utilized in this study. The equations analyzed are the simple equations of heat transfer.

Most recently Yang (19) at the University of Michigan has published work relating the response of various flow parameters to arbitrary time-varying flow rates. The heat transfer coefficient is assumed to vary as a power of the coolant velocity, and a perturbation technique similar to the one employed in this study is applied to obtain the results. Calculations are carried out to illustrate several types of flow transients.

Unfortunately the results apply only to the double-pipe and shell-tube type heat exchangers.

As the temperature of the heat transfer surface increases, the type of flow changes due to the various mechanisms occurring at the boundary. Much work is being done in two phase heat transfer, in boiling heat transfer, and in several related areas. Gamma radiation is being used to measure void fractions and slip velocities, while visual studies using high speed cameras are being made of the mechanisms of bubble formation. Work has been done along similar lines at Argonne National Laboratory with respect to the coolant channels of the research reactor, A^2R^2 (18). Weatherhead investigated the effect of a gradual change in the sub-cooling of the inlet water. This produced changes in flow regime, outlet temperature, pressure drop, and wall temperature, and eventually burnout of the electrically heated test sections. For further study into the fields of boiling and two phase heat transfer Kepple and Tung (12) have provided an annotated bibliography of articles relating to this field.

It may be seen from this survey that researchers have as their purpose the devising of the best means of representing a heat transfer system. For a forced convection, single phase system graphical and numerical techniques, although the simplest, are often not accurate enough to satisfy analysis requirements. More complicated theoretical methods have as yet not been adequately perfected, although the ever-increasing use and application of computer codes promise a large reduction in calculation time. Transfer function methods have often been used by control engineers and will continue to be used in the future.

3.0 THEORETICAL DEVELOPMENT

3.1 Time Behavior of the Wall Temperature

In order to arrive at a transfer function for an internally cooled, electrically heated, circular tube it is necessary to examine the temperature distribution in the wall of the tube itself. The derivation of this distribution is based on the following assumptions:

(a). Heat generation within the tube is uniform.

(b). Heat is conducted radially only; the outer surface is adiabatic.

(c). The thermal conductivity of the metal wall is constant and corresponds to that of the mean wall temperature.

Taking an elemental slice dz and performing a heat balance on an element of volume (Fig. 1) in that slice, produces

$$q_1 + q_4 = q_3 + q_2 \tag{1}$$

where q_1 equals heat out, q_4 is the energy stored as a temperature rise of the metal, q_3 is the heat transferred in by conduction, and q_2 is the heat generated per unit volume. Now q_1 can be expressed as

$$q_1 = k\, dA \frac{dt}{dr} = k\, r\, d\theta\, dz \frac{dt}{dr} . \tag{2}$$

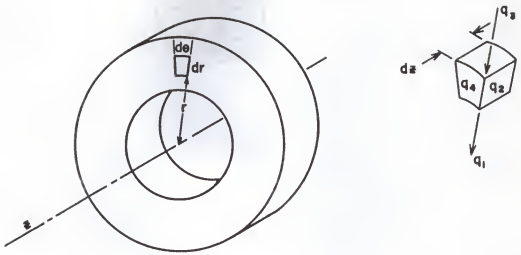

FIGURE I: GEOMETRY OF HEATED TUBE

Also

$$q_2 = dv\, q''' = q'''\, r\, dr\, d\theta\, dz, \tag{3}$$

and similarly q_3 can be written

$$q_3 = k\, dA \frac{dt}{dr} + \frac{d}{dr}\left(k\, dA \frac{dt}{dr}\right) dr. \tag{4}$$

The final quantity is

$$q_4 = dv\, \rho\, C_p \frac{dt}{d\tau}. \tag{5}$$

Substituting the above expressions into Eq. (1) and dividing through by k dv produces

$$q'''/k + \frac{1}{r}\frac{dt}{dr} + \frac{d^2t}{dr^2} = \frac{\rho C_p}{k}\frac{\partial t}{\partial \tau} \tag{6}$$

where $\rho C_p/k = \alpha^{-1}$. In the steady state condition $\frac{dt}{d\tau} = 0$ and Eq. (6) becomes

$$-q'''/k = \frac{1}{r}\frac{dt}{dr} + \frac{d^2t}{dr^2} \tag{7}$$

The general solution to this equation is

$$t = q''' r^2(4k)^{-1} + C_1 \ln r + C_2. \qquad (8)$$

Using the boundary condition that the pipe is adiabatic at its outer diameter, i.e. the derivative is zero at r_o, determines C_1. Assuming that the temperature is known at either the inside or outside diameter, C_2 can be solved for in terms of this temperature. Thus the expression for t becomes

$$t = t_o - q''' (2r_o^2 \ln \frac{r_o}{r} - r_o^2 + r^2) \cdot (4k)^{-1}, \qquad (9)$$

where t_o is the temperature of the wall at the outer radius.

3.2 Time Behavior of Coolant Temperature

In this section the means of describing the behavior of the coolant flowing in the tube is devised. In order to do this some simplifying assumptions are made:

(a). A mean temperature and average velocity of the fluid can be utilized with respect to radial direction.

(b). Axial heat conduction effects are negligible.

(c). The heat transfer coefficient is constant with z and proportional to $u^{0.8}$.

(d) The fluid is incompressible and all fluid properties are mean values evaluated at the average temperature between the inlet and the outlet.

(e). The temperature of the fluid entering the coolant channel is constant and equal to θ_o.

If the first law of thermodynamics is applied to the differential fluid volume, where the first law is expressed as

$$\frac{\partial}{\partial \tau} \int_V e \, dm + \int_A u \, (e + pv) \, dA = q - P_z \ldots, \tag{10}$$

the behavior of the system when kinetic energy and height changes are ignored is expressed as

$$\frac{\partial}{\partial \tau} (e\rho A) \, dz + \frac{\partial}{\partial z} (\rho u A \, H) \, dz \tag{11}$$

$$= h(t_i - \theta)\pi \, 2r_i \, dz + kA \, \frac{\partial^2 \theta}{\partial z^2} \, dz$$

Assuming that $kA \, \frac{\partial^2 \theta}{\partial z^2} \, dz$ is negligible and $C_p \triangleq C_v$ produces

$$(t_i - \theta) = \frac{\partial \theta}{\partial \tau} \rho C_p \, r_i/2h + \frac{\partial \theta}{\partial z} u\rho C_p \, r_i/2h. \tag{12}$$

In the steady state solution it is apparent that the heat transferred to the coolant must equal the heat generated in the tube wall. From this equality it can be shown that

$$t_i - \theta = q''' \, (r_o^2 - r_i^2) \, (2hr_i)^{-1} \tag{13}$$

and the expression for $\frac{d\theta}{dz}$ is

$$\frac{d\theta}{dz} = q''' \, (r_o^2 - r_i^2) \, (u\rho \, C_p \, r_i^2)^{-1}. \tag{14}$$

Upon integrating with the boundary condition $\theta(0) = \theta_o$ Eq. (14) becomes

$$\theta = \theta_o + z \, q''' \, (r_o^2 - r_i^2) \, (u\rho \, C_p \, r_i^2)^{-1}. \tag{15}$$

It is now convenient to define the constants:

$$a_1 = q''' \, (r_o^2 - r_i^2) \, (2r_i)^{-1} = q'' \tag{16}$$

$$a_2 = q''' \, (r_o^2 - r_i^2) \, (\rho \, C_p \, r_i^2)^{-1} \tag{17}$$

$$a_3 = a_1/a_2, \tag{18}$$

so that Eq. (12) becomes

$$t_1 - \theta = \frac{a_3}{h}\frac{\partial\theta}{\partial\tau} + \frac{a_3}{h} u \frac{\partial\theta}{\partial z}, \tag{19}$$

and θ can be expressed as

$$\theta = \theta_o + z\,(a_2/u). \tag{20}$$

For convenience Eq. (13) is rearranged to the form

$$t_1 = \theta + a_1/h = \theta_o + z\,(a_2/u) + a_1/h. \tag{21}$$

3.3 Application of the Perturbation Method

Equations (6) and (19) are linear but have variable coefficients h and u; therefore, the transfer function between coolant velocity and outlet coolant temperature is derived by means of a perturbation method with the assumption of small variations in coolant velocity and velocity dependent heat transfer coefficients. The steady state solutions have been derived and are Eqs. (9), (20), and (21).

If the temperature of the wall as described by Eq. (6) is to be described by some steady state component t plus an unsteady state perturbation component t' which is caused by a change in coolant velocity, then Eq. (6) becomes

$$\frac{q'''}{k} + \frac{1}{r}\frac{d(t + \varepsilon t')}{dr} + \frac{d^2(t + \varepsilon t')}{dr^2} = \frac{1}{\alpha}\frac{d(t + \varepsilon t')}{d\tau}. \tag{22}$$

Assuming that t' and t are independent and eliminating the steady state components in Eq. (22), the terms of order epsilon are

$$\frac{d^2t'}{dr^2} + \frac{1}{r}\frac{dt'}{dr} = \frac{1}{\alpha}\frac{dt'}{d\tau}. \tag{23}$$

Now performing a Laplace transformation with respect to time on Eq. (23) produces

$$(s/\alpha)\,\bar{t}' = \nabla^2\,\bar{t}'. \tag{24}$$

If a new variable $\mu = \sqrt{s/\alpha}\, r$ is defined, Eq. (24) becomes after multiplying by r^2

$$\mu^2 \bar{t}' = \mu \frac{d\bar{t}'}{d\mu} + \mu^2 \frac{d^2\bar{t}'}{d\mu^2} . \tag{25}$$

The solution to Eq. (25) is a combination of the modified Bessel functions of zero order, and is of the form

$$\bar{t}' = A\,(z,s)\, I_o\,(\mu) + B\,(z,s)\, K_o\,(\mu), \tag{26}$$

where the constants of integration are functions of time and axial position in this lumped parameter approach. Applying the boundary condition at the outside wall produces

$$\left.\frac{d\bar{t}'}{d\mu}\right|_{r = r_o} = A\,(z,s)\, I_1\,(\mu_o)\,(s/\alpha)^{\frac{1}{2}} - B\,(z,s)\, K_1\,(\mu_o)\,(s/\alpha)^{\frac{1}{2}} = 0 \tag{27}$$

so that

$$B = A\,(z,s)\, I_1\,(\mu_o)/K_1(\mu_o). \tag{28}$$

Eq. (26) then becomes

$$\bar{t}' = A\,(z,s)\,\{I_o(\mu) + K_o(\mu)\, I_1\,(\mu_o)/K_1(\mu_o)\}. \tag{29}$$

In order to proceed further, similar operations are performed on the equation describing coolant behavior; thus Eq. (19) becomes

$$\frac{h}{a_3}(t_1 - \theta) = \frac{\partial\theta}{\partial\tau} + u\frac{\partial\theta}{\partial z} . \tag{30}$$

Letting u equal $u + \varepsilon u'$ where u' is the change in coolant velocity, h equal $h + \varepsilon h'$ where h' is the change in the heat transfer coefficient due to the change in coolant velocity, and θ equal $\theta + \varepsilon\theta'$ where θ' is the change in coolant temperature; Eq. (30) produces

$$(h + \varepsilon h')\left\{(t + \varepsilon t') - (\theta + \varepsilon\theta')\right\}/a_3$$

$$= \frac{\partial\,(\theta + \varepsilon\theta')}{\partial\tau} + (u + \varepsilon u')\,\frac{\partial\,(\theta + \varepsilon\theta')}{\partial z}\,. \qquad (31)$$

Ignoring second order perturbations (ε^2) and making use of the equivalence evidenced in Eq. (30) to cancel out the steady state terms, the result is

$$h\,(t'_1 - \theta')/a_3 + h'\,(t_1 - \theta)/a_3 = \frac{\partial\theta'}{\partial\tau} + u\,\frac{\partial\theta'}{\partial z} + u'\,\frac{d\theta}{dz}\,. \qquad (32)$$

The second boundary condition is taken to be the assumption that the heat lost from the test section by conduction at r_1 equals the heat transferred by convection. Writing this in perturbation form and following previously outlined procedure to eliminate steady state components produces

$$k\,\frac{\partial t'_1}{\partial r}\bigg|_{r\,=\,r_1} = h(t'_1 - \theta') + h'\,(t_1 - \theta). \qquad (33)$$

Replacing $(t_1 - \theta)$ and $\frac{d\theta}{dz}$ in Eq. (32) by their initial steady state values given in Eqs. (21) and (20), produces

$$(t'_1 - \theta')\,h/a_3 + a_2\,h'/h = \frac{\partial\theta'}{\partial\tau} + u\,\frac{\partial\theta'}{\partial z} + a_2\,u'/u. \qquad (34)$$

It has been mentioned before that the heat transfer coefficient between the coolant and the tube is assumed to vary like the n power of the coolant velocity so that

$$(h + \varepsilon h')/h = (u + \varepsilon u')^n/u^n. \qquad (35)$$

Expanding and comparing coefficients of ε, one arrives at

$$h'/h = n\,u'/u, \qquad (36)$$

and Eq. (34) becomes

$$(t'_1 - \theta')\,h/a_3 + a_2\,n\,u'/u = \frac{\partial\theta'}{\partial\tau} + u\,\frac{\partial\theta'}{\partial z} + a_2\,u'/u, \qquad (37)$$

and similarly Eq. (33) becomes

$$k \left.\frac{\partial t'_1}{\partial r}\right|_{r = r_1} = h\,(t'_1 - \theta') + n\,h\,(t_1 - \theta)\,u'/u. \tag{38}$$

Substituting the initial steady state or unperturbed $(t_1 - \theta)$ gives

$$k \left.\frac{\partial t'_1}{\partial r}\right|_{r = r_1} = h\,(t'_1 - \theta') + n\,a_1\,u'/u. \tag{39}$$

The Laplace transform of Eq. (33) is taken and utilized with Eq. (29) to yield

$$h^{-1}A\,(z,s)\,k\,(s/\alpha)^{\frac{1}{2}}\,\{I_1\,(\mu_1) - E\,K_1\,(\mu_1)\} = A\,(z,s)\,\{I_o\,(\mu_1) + E\,K_o\,(\mu_1)\} - \overline{\theta}' + n\,a_1\,\overline{u}'\,(uh)^{-1}, \tag{40}$$

where E is $I_1\,(\mu_o)/K_1\,(\mu_o)$. Solving for $\overline{\theta}'$, one obtains

$$\overline{\theta}' = A\,(z,s)\,\{k\,(s/\alpha)^{\frac{1}{2}}\,h^{-1}\,E\,K_1\,(\mu_1) - I_1\,(\mu_1) + I_o\,(\mu_1) + E\,K_o\,(\mu_1)\} + n\,\overline{u}'\,a_1\,(uh)^{-1};$$

$$\overline{\theta}' = A\,(z,s)\,g_o\,(s) + n\,\overline{u}'\,a_1\,(uh)^{-1}, \tag{41}$$

and an associated relationship utilizing Eq. (29) is

$$\overline{t}'_1 - \overline{\theta}' = A\,(z,s)\,k\,(s/\alpha)^{\frac{1}{2}}\,h^{-1}\{I_1\,(\mu_1) - E\,K_1\,(\mu_1)\} - n\,\overline{u}'\,a_1\,(uh)^{-1},$$

or

$$\overline{t}'_1 - \overline{\theta}' = A\,(z,s)\,g_1\,(s) - n\,a_1\,\overline{u}'\,(uh)^{-1}. \tag{42}$$

The functions g_o and g_1 defined by Eqs. (41) and (42) are introduced for convenience. A Laplace transformation can now be applied to Eq. (37) which when utilized with Eq. (41) and Eq. (42) to form a differential equation for A (z,s) becomes

$$\{A\ (z,s)\ g_1 - n\ \bar{u}'\ a_1\ (uh)^{-1}\}\ h/a_3 + n\ a_2\ \bar{u}'/u$$

$$= s\ A\ (z,s)\ g_o + s\ a_1\ n\ \bar{u}'\ (uh)^{-1} + u\ g_o\ \frac{d\ A\ (z,s)}{dz} + a_2\ \bar{u}'/u, \qquad (43)$$

which yields when simplified

$$\frac{d\ A\ (z,s)}{dz} + A\ (z,s)\ \{s/u - g_1\ h\ (u\ a_3\ g_o)^{-1}\}$$

$$= -\bar{u}'\ a_2\ u^{-2}\ g_o^{-1} - s\ n\ \bar{u}'\ a_1\ u^{-2}\ (h\ g_o)^{-1}. \qquad (44)$$

Equation (44) can be solved for A (z,s) by the integrating factor method

$$A\ (z,s) = -f_1^{-1}\ \{\bar{u}'\ a_2\ u^{-2}\ g_o^{-1} + s\ n\ \bar{u}'\ a_1\ u^{-2}\ (g_o\ h)^{-1}\} + Ce^{-f_1 z}, \qquad (45)$$

where

$$f_1 = s/u - h\ g_1\ (a_3\ u\ g_o)^{-1}\ . \qquad (46)$$

The function $\bar{\theta}'$ now equals from Eq. (41)

$$\bar{\theta}' = -(f_1)^{-1}\ (\bar{u}'\ a_2\ u^{-2} + s\ n\ \bar{u}'\ a_1\ u^{-2}/h) + g_o\ Ce^{-f_1 z} + \frac{n\ \bar{u}'\ a_1}{uh} \qquad (47)$$

Using the boundary condition that $\bar{\theta}'\ (0,s) = 0$, the integration constant C can be evaluated as

$$C = +\{(\bar{u}'\ a_2\ u^{-2} + s\ n\ \bar{u}'\ a_1\ u^{-2}/h) f_1 - n\ \bar{u}'\ a_1\ (uh)^{-1}\}/g_o\ , \qquad (48)$$

and $\bar{\theta}'$ can be written

$$\bar{\theta}' = (e^{-f_1 z} - 1)\ (s\ n\ a_1 - n\ a_1\ f_1\ u + a_2\ h)\ \bar{u}'\ (u^2\ f_1\ h)^{-1}\ . \qquad (49)$$

The coolant temperature transfer function with respect to the coolant velocity is now

$$\frac{\overline{\theta}'}{\overline{u}'} = (e^{-f_1 z} - 1) \{n (s - u f_1) + h/a_3\} a_1 (u f_1 h)^{-} \qquad (50)$$

where f_1 is expressed for convenient calculation from Eqs. (41), (42) and (46) as

$$f_1 = s/u + h \{a_3 u \; 1 + h (a/s)^{\frac{1}{2}}/k (I_o (\mu_1) + E K_o (\; _1))$$

$$(E K_1 (\mu_1) - I_1 (\mu_1))^{-1} \}^{-1}. \qquad (51)$$

The equilibrium value or value of $\overline{\theta}'_L$ when time is infinite is found by utilizing the property of the Laplace transform illustrated in Eq. (52)

$$\lim_{s \to 0} s \overline{f} (s) = \lim_{t \to \infty} f (t) \qquad (52)$$

or

$$\theta'_L(\infty) = \lim_{s \to 0} s \cdot a_1 u' s^{-} (1 - e^{-f_1 L}) \{n (s - u f_1) + h/a_3\} \cdot$$

$$\cdot (u^2 f_1 h)^{-1} = u' a_1 L u^{-2}/a_3 = 2 u' q'' L (u^2 \rho C_p r_1)^{-1}. \qquad (53)$$

An exact theoretical solution yields, if u' is a negative step change,

$$\theta'_L(\infty) = 2 u' q'' L \{u (u - u') \rho C_p r_1\}^{-1}. \qquad (54)$$

The discrepancy is produced by the neglection of the second order terms of the perturbed velocity. For high velocity and/or small perturbations the error is negligible. Also for large temperature drops down the length of the tube this error will be negligible.

3.4 Transient Response

3.4.1 Coolant temperature-velocity transfer function approximation

The 1401-1410 IBM computer was used to calculate plots of the gain in decibels and the phase shift versus the logarithm of the normalized frequency for varying values of heat flux, initial velocity, and heat transfer coefficient. These curves are shown in Figs. 2 and 3, in the form of Bode plots. Series approximations utilizing the imaginary arguments were used to evaluate the Bessel functions. Machine and series limitations dictated that the calculations be made in three parts. The parameters utilized in this calculation are shown in Table I and are experimental values.

A visual straight line approximation was made by using multiples of 20 decibel/decade slopes to form the curve. These were adjusted by trial and error until the closest combination was found. The final approximate functions are shown in Figs. 2 and 3 as solid lines. Approximation (1) most closely follows the response of 0.200 and 0.220 fractional flow rates. Approximation (2) follows the curves of the higher flow rates.

No attempt was made to fit the curves past the 20 decibel attenuation point due to both the difficulty in fitting the oscillations and the fact that any exponentials of this magnitude would not be significant in the time response. The form of the approximated transfer function is

$$\bar{\theta}'/\bar{u}' = \theta'_L(\infty)\,(1 + s/\omega_1)\,\{u'\,(1 + s/\omega_2)\,(1 + s/\omega_3)\,(1 + s/\omega_4)^2\}^{-1}, \quad (55)$$

where the values of ω_j are given in Table II.

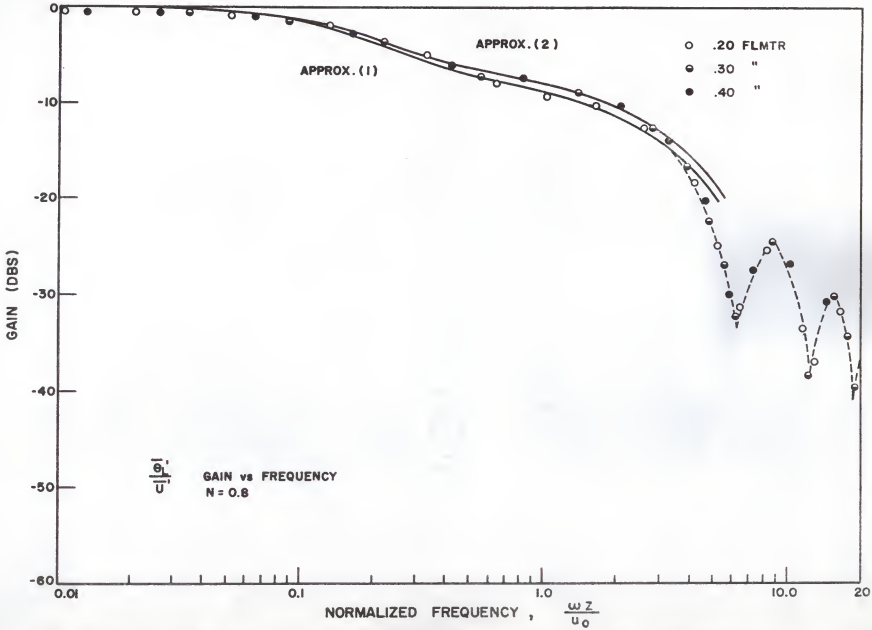

FIGURE 2: GAIN PLOT OF TRANSFER FUNCTION; CALCULATED AND APPROXIMATIONS

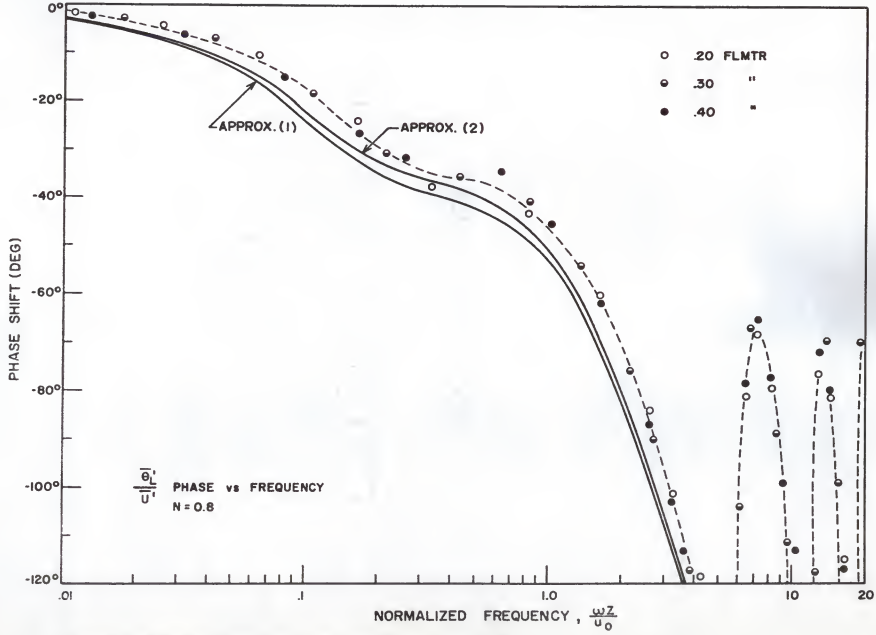

FIGURE 3: PHASE SHIFT PLOT OF TRANSFER FUNCTION

3.4.2 Coolant Temperature Transient Response

The value of the approximation given in section 3.4.1 can be made apparent by examining the response of the system to a step change in velocity. Applying the Laplace of a velocity step change and rearranging Eq. (52) produces

$$\bar{\theta}'_L \pm u' \, (1 + s/\omega_1) \cdot \{(s + \omega_2)\,(s + \omega_3)\,(s + \omega_4)^2\}^{-1}. \quad (56)$$

By the method of partial fractions and the application of inverse Laplace transformations, the transient response can be shown to be

$$\theta'_L(\tau) = \theta'_L(\infty) \cdot (1 + W_2\, e^{-\omega_2 \tau} + W_3\, e^{-\omega_3 \tau} + W_4\, e^{-\omega_4 \tau} + \tau W_5\, e^{-\omega_4 \tau}), \quad (57)$$

where the necessary values are tabulated in Table II. The solution to the actual time response would involve the inversion of Eq. (50) with a multiplicative factor of $\bar{u}'/s$; a difficult and tedious process. This would be virtually impossible to achieve analytically and difficult to program. Approximations have been made by previous investigators in the integration of the frequency response to predict transient behavior, but these do not provide a significantly more accurate solution.

3.5 Thermocouple Behavior

Before the theoretical response can be compared to experimental data some corrections must be made with regard to the response of the thermocouple and its associated mass. The response is assumed to be of first order but with a slowly varying time constant (c) and a slowly decreasing

Table I. Constants for computer calculation of transfer function.

Stainless steel

density (ρ)	501 lbs-ft^{-3}	inner radius (r_i)	.01041 ft.
heat capacity (C_p)	.12 Btu/lb$_m$ ^{o}F	outer radius (r_o)	.02082 ft.
		heated length (L)	4.00 ft.

Fractional flow rate	K_{ss} * (Btu/hr ft ^{o}F)	H_2O * (lbs/ft^3)	u_o * (ft/hr)	C_p * (Btu/lb ^{o}F)	h † (Btu/ft ^{o}F)	q'' † (Btu/hr ft^2)
0.20	9.33	61.6	19,300	0.99	1161	1.3×10^5
0.30	8.96	61.8	28,900	0.99	1520	1.3×10^5
0.35	9.83	61.6	33,800	0.99	1710	2.6×10^5
0.40	9.74	61.6	38,600	0.99	1836	2.6×10^5
0.535	10.0	61.6	51,700	0.99	2341	3.9×10^5

* These properties were calculated by interpolating in the tables of thermal properties in reference 11.

† Calculated from experimental data.

Table II. Constants of exponential series approximations.

$\omega_j = (\text{sec})^{-1}$

approximation 1, $\omega_1 = 0.1\ u_o$; approximation 2, $\omega_1 = 0.09\ u_o$

$\omega_2 = .0375\ u_o\ (\text{sec})^{-1}$ $\quad W_2 = (\omega_2\omega_3\omega_4^2/\omega_1)\ (1 - \omega_1/\omega_2)(\omega_3\omega_2)^{-1}(\omega_4-\omega_2)^{-1}$

$\omega_3 = u_o$ $\quad W_3 = (\omega_2\omega_3\omega_4^2/\omega_1)\ (1 - \omega_1/\omega_3)(\omega_2 - \omega_3)^{-1}(\omega_4-\omega_3)^{-1}$

$\omega_4 = 1.125\ u_o$ $\quad W_4 = -\ 1 - W_2 - W_3$

$W_5 = (\omega_2\omega_3\omega_4^2/\omega_1)\ (1 - \omega_1/\omega_4)(\omega_2 - \omega_4)^{-1}(\omega_3 - \omega_4)^{-1}$

steady state error (a/c). These effects are due to time dependent conduction losses along the thermocouple wires (9). For the purposes of analysis a and c are assumed to be constant over the time interval considered.

The thermocouple and its construction is described in detail in the maintenance manual to the loop (5). In order to test its transient response it was removed from its installation. The couple was tested by rapid immersion in a hot water bath. The response was recorded in the form of a trace by an E. A. I. x-y plotter. The approximate transfer function of the couple was multiplied by that of the expected response of the system and the result inverted by partial fraction techniques into a series of exponentials. The approximate transfer function of the thermocouple was found to be of the form

$$\bar{\theta}_m/\bar{\theta}' = a/(s + c) \tag{58}$$

where θ_m is the measured temperature response. The constants were found from plots of the response of the thermocouple to immersion (Fig. 4) and used in the machine calculation of the expected response of the test section.

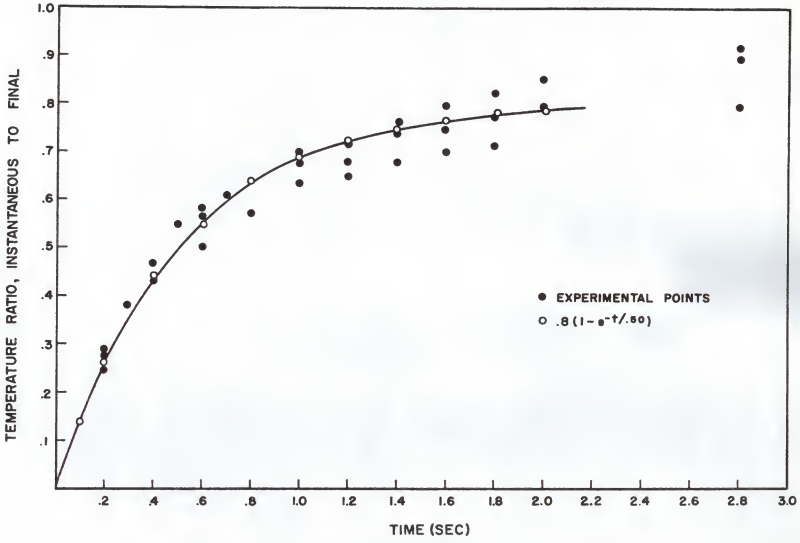

FIGURE 4: THERMOCOUPLE RESPONSE TO IMMERSION

4.0 EXPERIMENTAL PROCEDURE

The heat transfer loop used to provide experimental data for this paper is described in detail in Appendix I. Since the loop was not designed for transient studies, modifications were made to permit the insertion of a step change in the velocity of the coolant flowing in the loop. The network which was installed for this purpose is shown in Fig. 5. This arrangement of parallel valves, one operated by a solenoid, enabled the velocity to change from full flow to a preset value with a minimum of oscillation. The exact insertion time of the input signal was displayed by monitoring the voltage to the solenoid valve. A visual check was provided by a flowmeter (FI-1) installed in the stream between the valves and the test section.

Due to a.c. pickup in the thermocouples of the test section, measurement of test section wall temperature was limited to steady state measurement by a Honeywell 24-channel continuous balancing recorder. The output or outlet coolant temperature was measured by an immersed, ceramo-type, chromel-alumel thermocouple connected for display to an x-y recorder equipped with a built-in time based signal generator for the x-axis. This recorder was equipped with a 60 cycle a.c. filter and provided a continuous record of the behavior of the outlet coolant temperature versus time. Since the solenoid valve was of the normally closed type, the exact experimental procedure followed consisted of the items listed below:

(a). Adjustment of the loop to the final conditions desired.

(b). Activation of the time-based recorder.

(c). Application of the voltage to the solenoid, opening the valve. At this point the loop must be allowed to come to its equilibrium value.

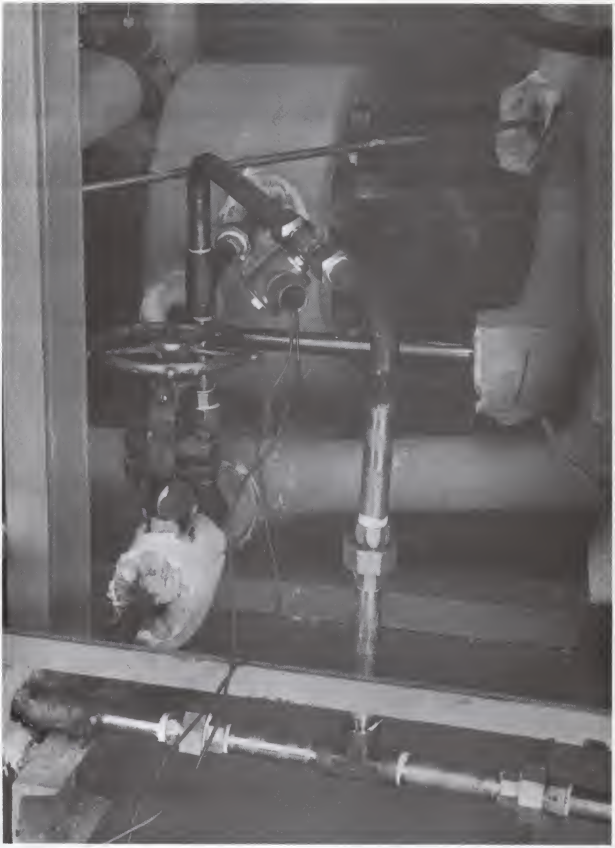

FIGURE 5 : PARALLEL VALVES TO ALLOW STEP INSERTION

(d). Cut-off to the solenoid closing the valve and the start of the time generating signal.

(e). De-activation of the time based recorder.

The curves of the outlet temperature were corrected for the time constants of the recorder and the transport lag of the fluid which slow the response. The time constant of the recorder was found by subjecting it to step inputs of voltage of the magnitude of the output signal and observing the 1/e time of the response. The transport lag is the time for the velocity wave to get to the test section from the valve and is easily computed. Actual traces of the plotter response to step changes of voltage input are shown in Fig. 6.

In the design of this experiment, care was taken to prevent sub-cooled boiling in the tube. The critical parameter was the inside wall temperature of the tube. This temperature was not permitted to exceed the boiling point of water at 300 psia or 417^{o}F. Parameters of the runs in this experiment are below in Table III.

Table III. Parameters of experimental runs.

POWER	FRACTIONAL FLOW RATE		PRESSURE
	INITIAL	FINAL	
30 kw	0.535	0.480	300 psia
20	0.400	0.340	300 psia
20	0.350	0.295	300 psia
20	0.340	0.280	300 psia
10	0.300	0.230	300 psia
10	0.220	0.140	300 psia
10	0.200	0.125	300 psia

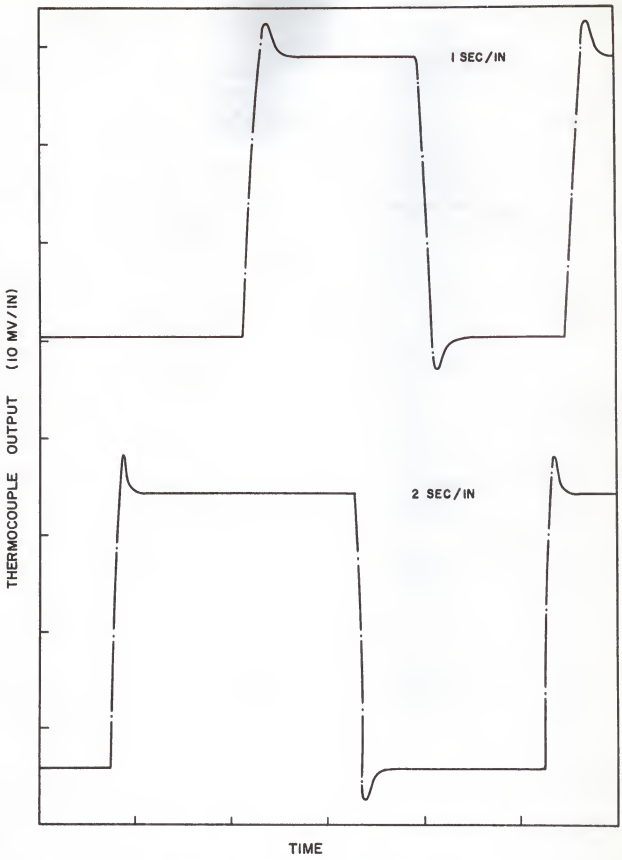

FIGURE 6: RECORDER RESPONSE TO STEP INPUTS

The determination of these parameters was experimental in nature and consisted of adjusting the power to a value, then decreasing the flow rate until the maximum non-boiling wall temperature was reached. Calculations were made to determine the difference between the measured or outer temperature and the significant inner wall temperature. Other flow rates were selected above the minimum flow rate to provide differing values of temperature perturbation.

5.0 RESULTS AND DISCUSSION

5.1 Results

Illustrated in Fig. 7 are actual traces of a series of thermocouple transients. It is apparent from a study of the response of the x-y plotter that its response time is small and may be neglected. The initial plateau of each trace represents the transport lag and can be seen to vary for each velocity. A correlation of these values reveals a characteristic length between valve and thermocouple of 18.8 ± 0.6 feet. The uncertainty is most probably due to the delay in closing the valve and the start of the time generating signal of the plotter. Also there is an inherent uncertainty in the reading of values from the graph of approximately ± 0.1 seconds.

Figure 8 shows the scatter of experimental points on the response curve for various values of initial velocity. In theory the responses for all velocities should fall on the same curve. In practice scatter is observed not only for a single velocity at a certain point but for various velocities. The maximum uncertainty at any point is $\pm .05 \frac{\theta(\tau)}{\theta(\infty)}$. This observed variation is due to the natural non-linearity of the system and uncertainties in transferring the data. The trend appears for the higher velocities to have a steeper response curve than the lower velocities, due to both the non-linearity of the system and the lesser dependence of the thermocouple transfer function on initial velocity. Also in Fig. 8 are the approximations to the transient response derived from the perturbation model.

Calculations of the final temperature have been made according to

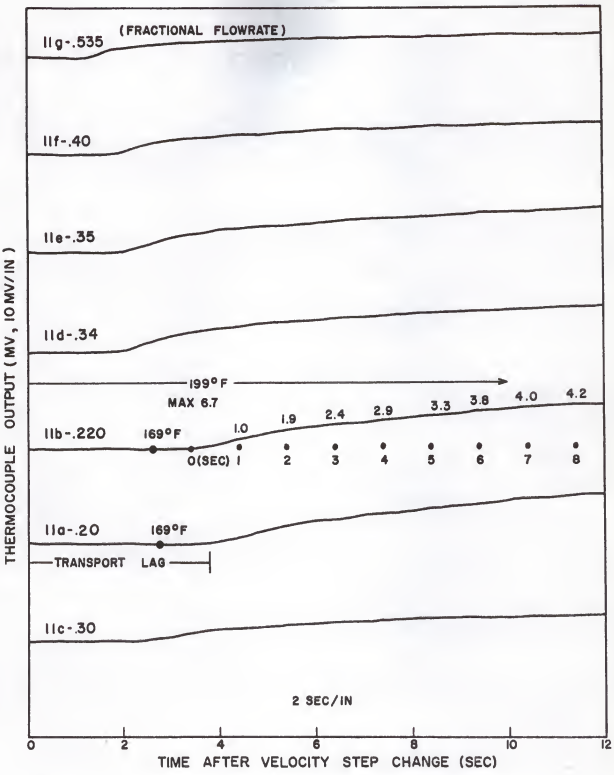

FIGURE 7: THERMOCOUPLE TRANSIENTS FOR VARIOUS INITIAL VELOCITIES

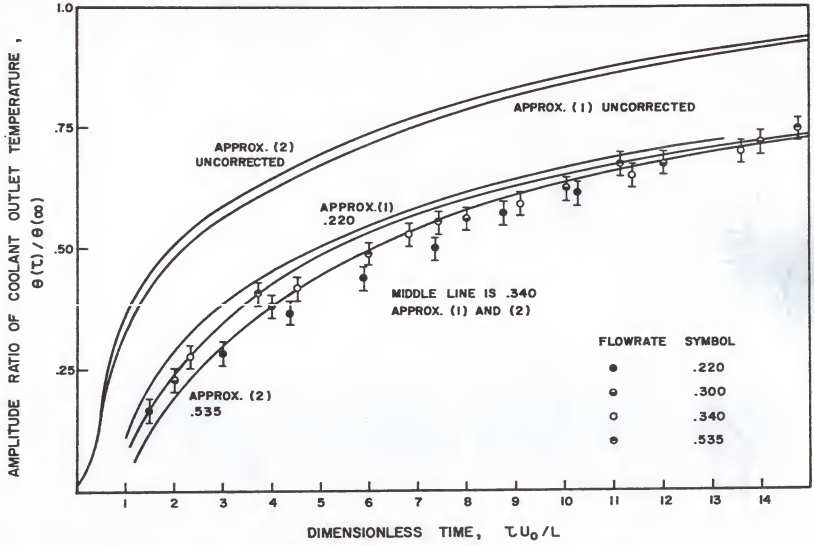

FIGURE 8: THEORETICAL AND EXPERIMENTAL TRANSIENT RESPONSE

Eqs.(53) and (54) and are compared with experimental values in Table IV. Study of these results reveals that the final temperature of the fluid can be calculated to ± 4 degrees F. assuming all errors occur only in the computation of the final perturbed condition.

5.2 Discussion

A careful study of the plots of the transfer function, Figs. 2 and 3, reveals the almost total dependence of the transfer function on initial flow rate. Calculations have been made with n = 0.7 which produce similar variations at the knee of the gain curve indicated as $0.1<\omega x/u_o<1.0$; thus destroying the belief that these variations are the result of an improper selection of n. This non-linear dependence on initial flow rate is not significant, however, when computing the transient response. This is demonstrated in Fig. 8 by the two uncorrected responses of Approx.(1) and Approx.(2). These curves reveal both the fact that the response is faster at higher velocities, and that the dependence of ω_1 on u_o is only approximately of first order. It should be noted that these curves are plotted versus a dimensionless time proportional to the velocity, and therefore the curves would not be the same when plotted versus real time. The experimental data reflects this non-linear dependence on flow rate and illustrates the general tendency of the responses of the higher flow rates to lie above the responses of the lower flow rates.

The plots of gain and phase shift also show the characteristic oscillations of a distributed parameter system subjected to a distributed disturbance. The physical significance of these resonances can be illustrated by considering a transient sinusoidal velocity producing a transient temperature re-

Table IV. Comparison of theoretical and experimental determination of outlet coolant temperature.

Power	Velocity(ft/hr) initial	final	u'	Outlet Temp.(^{o}F) initial	final	Experimental $\theta_L^i(\infty)^{o}$F	Eq. (53) $\theta_L^i(\infty)^{o}$F	Eq. (54) $\theta_L^i(\infty)^{o}$F
10 kw	19,300	12,550	6,750	175	218	43	30	45
	19,300	12,550	6,750	167	210	43	30	45
	19,300	12,550	6,750	178	221	43	30	45
	19,300	12,550	6,750	180	219	39	30	45
	19,300	12,550	6,750	169	208	39	30	45
	19,300	13,500	5,800	175	208	33	25	36
	19,300	13,000	6,300	170	205	35	28	41
avg.		12,750	6,550			39	29	43
10 kw	28,900	24,000	4,900	145	162	17	9.5	11.5
	28,900	24,000	4,900	142	155	13	9.5	11.5
	28,900	24,500	4,400	145	157	12	9	10
	28,900	22,100	6,800	142	160	18	13	17
	28,900	22,100	6,800	150	165	15	13	17
	28,900	22,100	6,800	141	157	16	13	17
	28,900	21,200	7,700	176	194	18	15	20
avg.		22,800	6,100			16	12	15
10 kw	33,800	29,500	4,300	132	142	10	6	7
20 kw	33,800	30,000	3,800	185	208	23	10	12
	33,800	30,000	3,800	186	209	23	10	12
	33,800	28,500	5,300	194	218	24	15	18
	33,800	28,500	5,300	194	218	24	15	18
	33,800	28,500	5,300	188	212	24	15	18
	33,800	28,500	5,800	190	217	27	16	20
Avg.		29,000	4,900			24	14	16
20 kw	38,600	32,800	5,800	175	191	16	12.5	15
	38,600	32,800	5,800	180	198	18	12.5	15
	38,600	32,800	5,800	180	198	18	12.5	15
	38,600	32,800	5,800	180	199	19	12.5	15
	38,600	34,700	3,900	170	187	17	8	10
	38,600	32,400	6,200	179	198	19	14	16
Avg.		33,000	5,600			18	12	15

sponse in a particle in the coolant stream. At the times $\omega\tau = 2\pi, 4\pi, \ldots, 2n\pi$ or the distances $\omega z/u_o = 2\pi\ldots$, the temperature of the particle will go through a minimum, where ω is the frequency of the sinusoidal oscillation.

Examination of Fig. 7 illustrates the difficulties involved in transferring the data. Runs c, f, and g were difficult to analyze due to the small magnitude of the total response. Run 11 b illustrates the method of analysis that was employed. The difficulty in obtaining the zero or starting point should be observed for the smaller velocities. It should also be noted that the left hand border represents the closing of the solenoid valve, or the insertion of the velocity change.

However, this analysis has provided an analytical expression that can be used to evaluate the transient response of the outlet coolant temperature of the test section of the heat transfer loop to various inputs expressible in Laplace transformations. The use of transfer function techniques coupled with theoretical analysis has been illustrated for several initial velocities subjected to a negative step change of velocity. The dependence of this response on initial velocity is best shown by the use of a dimensionless frequency $\omega z/u_o$ to plot both gain and phase shift and the use of a dimensionless time $\tau\, u_o/z$ to plot response curves. The large discrepancies between the theoretical and experimental response curves for the fractional velocities below 0.340 can in part be accounted for by the inapplicability of the perturbation theory to conditions where the change is a considerable percentage of the original flow rate. The transfer function and associated response calculated for an initial flow meter reading of 0.535 was found to be most adequate and provided the best approximation to the experimental data.

The weak point in the approximated transfer function lies in the evaluation of the thermocouple response. In the approximation of this study, the couple is immersed in a hot water bath and the response observed. The transfer function of the thermocouple is estimated and applied to the uncorrected transfer function of outlet temperature by transfer function multiplication. The response of the corrected transfer function is evaluated to produce the corrected curves shown in Fig. 8. The error in this assumption is due to the difference in the heat transfer coefficient in the bath and in the flow stream. The time constant (c) is derived from theoretical considerations to be proportional to the heat transfer coefficient which is proportional to the 0.44 power of velocity for flow transverse to horizontal cylinders. However, actual tests (9) with Chromel P-Alumel thermocouples dropped into fluid jets of varying velocities, produced no specific changes in the time constant. From this the authors concluded that the dominant factor of the response is the mass of the thermocouple bead. This assumption is used in this thesis to justify the use of a velocity independent thermocouple transfer function.

6.0 SUGGESTIONS FOR FURTHER STUDY

The heat transfer loop used in this thesis although limited for transient study, is quite versatile in two other respects. With certain modifications in the electric alarm and safety system, the loop can be operated in the free or natural convection mode. This thermal siphoning effect caused by the difference in densities at the top and bottom of the test section is accomplished by shortcircuiting the pump and by-passing it by means of a valve provided for that purpose. The electrical modifications needed are described briefly in Appendix III. This natural circulation mode has not been investigated as thoroughly perhaps as the forced convection mode, and valuable contributions could be made in the predictions of flow rates, pressure drops, friction factors, and film coefficients for various values of heat generation, especially with regard to this device.

A wide field of possibilities is available for different test section geometries. This would require more modification and more time than natural circulation studies but holds more promise for the solution of problems relating to unusual fuel element shape. Rectangular sections simplify the geometry and have been fairly well investigated. Triangular test sections pose new problems due to the formation of hot spots and unusual temperature distributions. Theoretically, test sections could be designed, built and installed according to a specific program as long as it did not involve boiling or two-phase study and/or transient analysis.

Although boiling can occur in the loop it does not represent a safe condition and will probably cause burnout of the test section. The heat exchanger is inadequate to deal with the production of the steam and the rise in the system pressure with the inception of boiling would cause an

automatic shutdown of the loop unless the safety alarm system were altered.

Transient analysis capabilities are limited because the a.c. power used to heat the test section produces an a.c. voltage and an a.c. current in the thermocouples used to monitor temperatures. A high speed or short response time recorder will oscillate with this current. The instruments currently measuring test-section temperature are continuous balancing, slow response instruments, adequate for only steady-state measurements. With the development of better instruments to filter out a.c. noise, transient analysis would be possible.

The alternative and the usual solution to this problem is a d.c. power source of sufficient magnitude to heat the test section. Unfortunately this would require insulation of the test section flanges since the grounding choke would no longer serve to prevent sizable current flow in the rest of the loop. Also the present control systems, which use a d.c. control on a saturable core reactor to control the a.c. power, would have to be drastically altered.

The heat transfer loop then functions well as a tool for use in an elementary heat transfer laboratory or for steady state study of forced and natural convection. It would not be suited for work in the two phase regime or for detailed transient studies without further modifications in instrumentation or power source.

7.0 ACKNOWLEDGEMENT

The author wishes to express his gratitude to Dr. J. O. Mingle for his advice, helpful suggestions and encouragement throughout the course of this study. Sincere appreciation is given to Dr. W. R. Kimel for his constructive criticism and encouragement. Special thanks must be extended to the Kansas State University Computing Center staff for their assistance, and recognition should be given to the Kansas State University Experiment Station for their financial support of this study.

8.0 LITERATURE CITED

1. Arpaci, V. S. and J. A. Clark
   Dynamic Response of Heat Exchangers Having Internal Heat Sources, Part I. J. Heat Transfer, 81, 253-266, Nov., 1959.

2. Ball, S. J.
   Simulation of Plug-Flow Systems. Instr. Cont. Systems, 36 133-49, Feb., 1963.

3. Ball, S. J.
   Approximate Models for Distributed Parameter Heat Transfer Systems. ISA Trans., 13, 38-47, 1964.

4. Canadian Westinghouse Co., Ltd.
   Light Water Heat Transfer Loop Operation and Maintenance Manual. Oct., 1959.

5. Canadian Westinghouse Co., Ltd.
   Light Water Heat Transfer Loop Maintenance Manuals and Instrument Sheets. Oct., 1959.

6. Colburn, A. P.
   A Method of Correlating Forced Convection Heat Transfer Data and a Comparison with Fluid Friction. Trans. AIChE, 19, 1933.

7. Dusinberre, G. M.
   Calculation of Transient Temperatures in Pipes and Heat Exchangers by Numerical Methods. Trans. ASME, 176, 1964.

8. Eckman, P. E.
   Industrial Instrumentation. New York: John Wiley and Sons, 1950.

9. Green, S. J. and T. W. Hunt
   Accuracy and Response of Thermocouples for Surface and Fluid Temperature Measurements. Temperature--Its Measurement and Control in Science and Industry, Part 2, 3, 1962.

10. Gyftopoulos, E. P. and J. B. Smets
    Transfer Functions of Distributed Parameter Nuclear Reactor Systems. Nuclear Science and Engineering, 5, 405-414, 1959.

11. Hoag, J. Barton
    Nuclear Reactor Experiments. New York: D. Van Nostrand, 1958.

12. Kepple, R. R. and T. V. Tung
    Two Phase (Gas-Liquid) System: Heat Transfer and Hydraulics, An Annotated Bibliography. ANL6734, July, 1963.

13. Quandt, E. R. and E. W. Fink
Experimental and Theoretical Analysis of the Transient Response of Surface-bonded Thermocouples. WAPD-BT-19, June, 1960.

14. Rhode, R. R.
The Methods and Apparatus Used in the Experimental Determination of Water Film Coefficients. School of Nuclear Science and Engineering, ANL Exp. 1, June, 1953.

15. Rizika, J. W.
Thermal Lags in Flowing Incompressible Fluid Systems Containing Heat Capacitors. Trans. ASME, 178, 1407, 1956.

16. Takahashi, Y.
Transfer Function Analysis of Heat Exchanger Processes. Automatic and Manual Control, Butterworths Scientific Publications, 235-248, 1952.

17. Takahashi, Y.
You Need No Computers to Graphically Determine the Dynamics of Heat Percolation. Control Engg., 2, 46-50, May, 1955.

18. Weatherhead, R. J.
Heat Transfer, Flow Instability, and Critical Heat Flux for Water in a Small Tube at 200 PSIA. ANL 6715, June, 1963.

19. Yang, W.
Transient Heat Transfer in a Vapor-Heated Heat Exchanger With Arbitrary Time-Wise Variant Flow Perturbation. Journal of Heat Transfer, 86, 133, May, 1964.

9.0 APPENDICES

9.1 APPENDIX A: HEAT TRANSFER LOOP

9.1.1 Main Loop System

The heat transfer loop is a thermodynamic system for measuring heat transfer coefficients of forced and natural convection, pressure drop, and other parameters of both an electrically heated test section, and the process water which is circulated in the loop. A schematic of loop flow is shown in Fig. 9. The dark, heavy line with arrows indicating the direction of flow in forced convection is the main loop. The pump is shown in the lower left-hand corner and the flow is counter-clockwise through V-1, a gate valve that regulates the flow, across FI-1, a flow meter for the main loop, and through V-2, another valve. It then enters the grounding choke, and goes to the test section. There it is heated by resistance heating of the stainless steel test section. The water then passes through V-3 to a shell-tube type heat exchanger. The heat exchanger is equipped with a by-pass valve V-4 in order to allow the operator to vary the temperature out of the heat exchanger. This process results in increasing the inlet temperature of the coolant to the test section. The two streams leaving the heat exchanger are mixed in the interchanger and return to the pump completing the cycle.

Both the pump and the heat exchanger are cooled by tap water and are connected to the water supply of Ward Hall. Means are provided for using this water in the loop but the deionizer provided for cleaning tap water did not prove efficient and a special distilled water line was installed with entry through V-22.

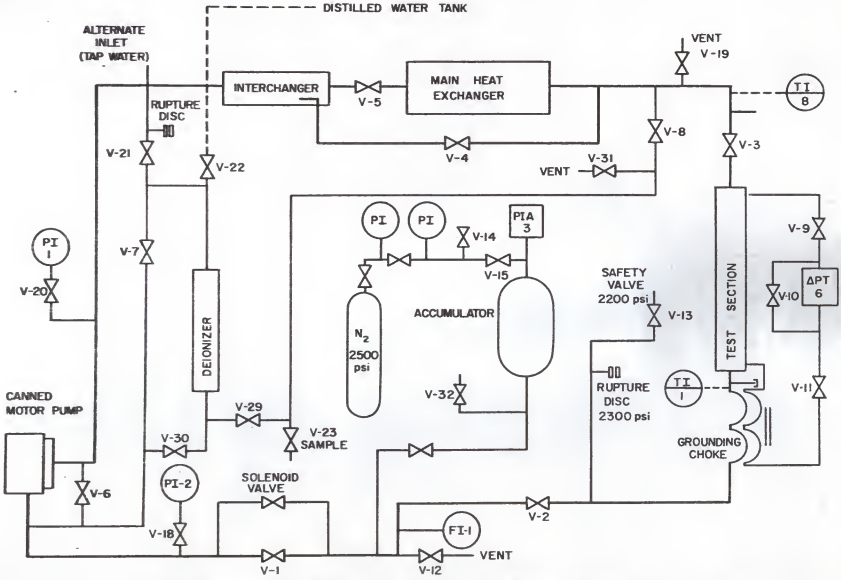

FIGURE 9 : SCHEMATIC OF PRESSURIZED-WATER HEAT TRANSFER LOOP

Consisting as it does of ½" stainless steel 347 schd. 80 pipe, the main loop piping is not very susceptible to corrosion, nor is the test section (316 stainless steel). The loop is covered with insulation providing limited access to the piping itself. The internal assembly or sub-loops is of ¼" stainless steel tubing and contains the deionizer, pressure gauges, safety valve, rupture discs, and the accumulator. This latter device maintains the pressure in the loop. It consists of a diaphram inflated with nitrogen to a specific pressure. The loop is designed to operate between the limits of 50 - 2500 psia.

9.1.2 Power Supply and Electrical System

The test section is heated by means of a 240 volt, 60 cycle supply controlled by an 800 amp., 2-pole circuit breaker CB-1. This breaker is closed only manually but is tripped automatically by an unsafe condition in the loop. In series with the 50/240 170 KVA transformer T-1, is a saturable core reactor controlled by means of a variable d.c. current produced by a variac. The output of the transformer is fed directly to the test section and is used to heat the tube. This arrangement is illustrated in Fig. 10. Instrumentation is provided to measure voltage (V-1), current (A-1), and power (W-1) applied to the test section.

To avoid the complication of insulating the test section flanges, one end of the test section is grounded. The pipe connected with the other end of the test section is twice passed through a laminated core before being connected to a ground. Sufficient current flows in this pipe to produce a voltage drop across it equal to the applied test section voltage. The pipe and

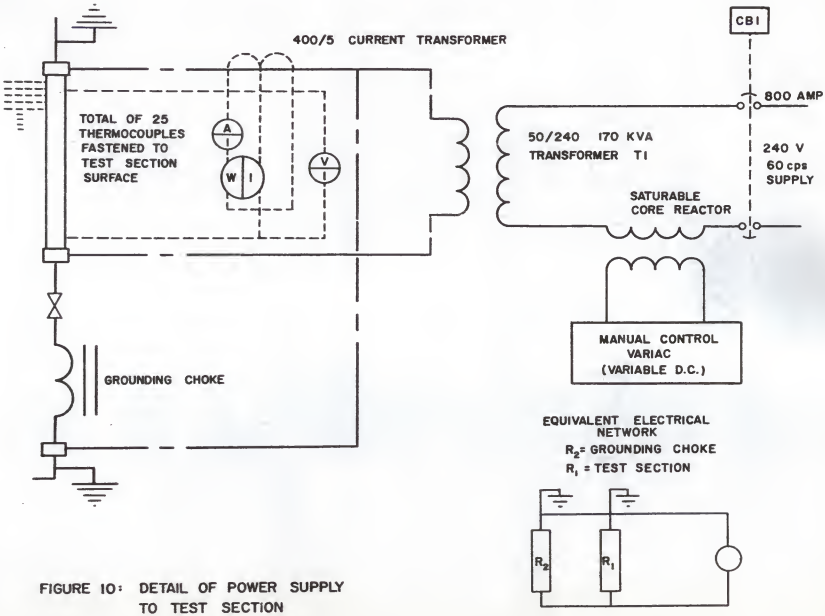

FIGURE 10: DETAIL OF POWER SUPPLY TO TEST SECTION

magnetic core form a high impedance choke so that a relatively small current will produce the required voltage drop. This current is indicated by A-3. A large cable connects the grounded end of the choke to the grounded end of the test section to insure that no current can flow in other parts of the loop.

A 40 amp., 3-pole circuit breaker controls the 240V, 3 phase, 60 c.p.s. supply to the loop auxilliaries. The pump is fed at this voltage through contactor C-2. Power control and instrumentation is obtained from the secondary of a 350 VA, 240/120 volt, control transformer.

9.1.3 Instrumentation and Control

All instruments are tabulated and described according to location, service, function, normal operating reading, control setting, alarm and/or trip setting (4).

Temperature

TI-1 Honeywell Millivoltmeter Pyrometer
Instr. Sheet #3 (5)
Location - Instrument control panel (see Fig. 11)

Service - Main Loop Water

Range - 0 - 800°F

Function - To indicate temp. of loop water at inlet to test section

Normal Reading - depends on experiment

TIA-2 Honeywell Protecto-O-Vane
Instr. Sheet #1
Location - Instrument control panel

Service - Main loop water

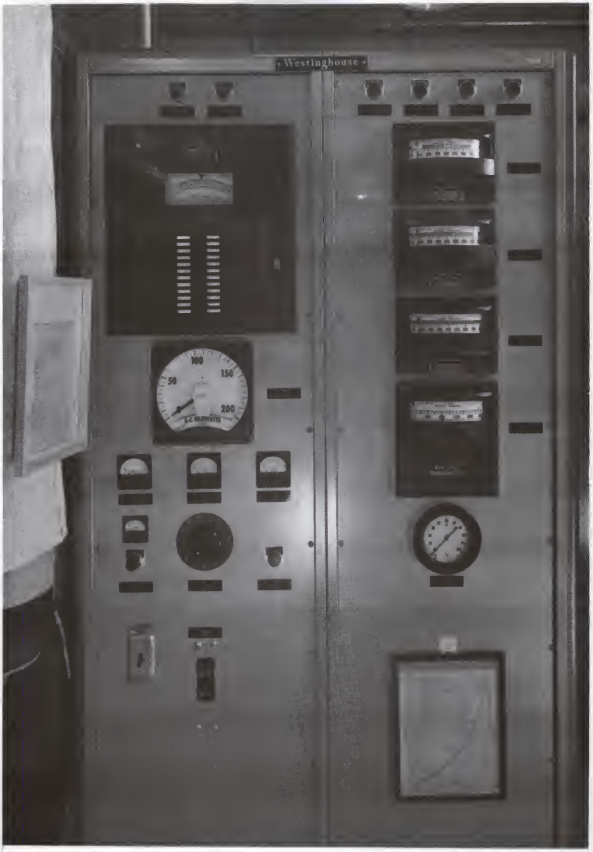

FIGURE II : CONTROL PANEL OF LOOP

Range - 0 - 2000°F

Function - to protect against overheating the test section by shutting off the test section heater and alarming

Trip setting - dependent on experiment
contacts TIA 2-1 open on loop temp. high, TIA 2-2 close on loop temp. high

Associated items - thermocouple TE-2, instr. sheet #4 welded to test section

TI-3 Honeywell 24 Point Precision Indicator
Instr. Sheet #2
Location - Instrument Panel

Service - Test section

Range - 0 - 1200°F

Function - To indicate temperature at various points on the test section

Normal Readings - dependent on experiment

Associated items - 24 chromel - alumel thermocouples TE-3-1 to TE-3-24, Instr. Sheet #4 welded to test section

TI-4 Moeller Bimet Dial Thermometer
Instrument Sheet #11
Location - In process water at outlet of heat exchanger

Service - Process water

Range - 0 - 250°F

Function - To indicate temperature of process water at heat exchanger outlet

Normal Reading - Approx. 150°F

TA-5 Fenwall Thermoswitch
Instr. Sheet #12
Location - In process water at outlet of heat exchanger

Service - Process water

Adjustable Range - 50 - 300°F

Function - to protect against malfunctioning of heat exchanger

Alarm setting - contacts close on temperature rise above 200°F

TC-6 Thermoswitch - supplied as integral part of canned motor pump
Location - embedded in motor stator winding

Function - To protect motor from overheating by tripping contactor

Control setting - contacts open on rising temperature as set by pump manufacturer

TI-8 Honeywell Millivoltmeter Pryometer
Instr. Sheet #2
Location - Instrument control panel

Service - Main loop water

Range - 0 - 1200°F

Function - Indicates main loop temperature at outlet of test section

Associated items - Thermocouple TE-8, Instr. Sheet #7, located at outlet of the test section

Flow

FI-1 F & P Armoured Flowrator Meter with overmounted magnetic indicator
Instr. Sheet #9
Location - in main loop piping between pump and inlet to test section

Service - Main loop water

Range - .4 to 4 gpm (a) 60°F & 2,500 psia

Function - to indicate main loop flow (Refer to graph mounted on control panel for scale factors at various temperatures)

Normal Reading - depends on experiment

FI-2 Fisher and Porter Indicating Flow rator
Instr. Sheet #10
Location - Process water at inlet to main heat exchanger

Service - Process water

Range - 1.3 to 16 gpm

Function - to indicate flow of process water through the heat exchanger

Normal reading - depends on experiment

FC-3 Fisher & Porter Ratosight Alarm
Instr. Sheet #13
Location - Main pump cooling water outlet

Service - process water

Range - .2 to 3 gpm

Function - to protect the main loop pump by de-energizing pump motor on low coolant flow

Setting - contacts open on decreasing flow below .25 gpm (adjustable)

Pressure

PI-1 Ashcroft Pressure Gauge
Instr. Sheet #5
Location - On main loop piping at inlet to pump

Service - Main loop water

Range - 0 - 3000 psia

Function - to indicate pump inlet pressure

Normal Reading - depends on experiment

PI-2 Ashcroft Pressure Gauge
Instr. Sheet #5
Location - On main loop piping at outlet of pump

Service - main loop water

Range of Instrument - 0 - 3000 psia

Function - to indicate pump outlet pressure

Main Reading - depends on experiment

PIA-3 Foxboro Pressure Indicator with high and low alarm contacts,
Instr. Sheet #8
Location - Inlet of accumulator

Service - Nitrogen

Range - 0 - 3000 psia

Function - measures nitrogen pressure at accumulator inlet and alarms on high and low pressure

Normal Reading - depends on experiment

High alarm setting - to open at 100 psi. above the selected normal value of PI-2

Low alarm setting - to open at 100 psi. below the selected normal value of PI-2

PI-4 Ashcroft Pressure Gauge Model 1279
Instr. Sheet #15
Location - In loop piping in process water supply

Service - in process water

Range - 0 - 160 psig

Function - to indicate process water supply

PI-6 Ashcroft Receiver Gauge
Instr. Sheet #6
Location - Instrument panel

Service - main loop water

Scale - 0 - 100% (3 - 15 psig)

Function - to indicate pressure drop across test section

Associated items - d/p transmitter PT-6

PT-6 Republic Differential Pressure Transmitter
Instr. Sheet #14
Location - in loop piping across the test section

Service - main loop water

Range - 75 psid. (Adjustable F.S.D. span from 16 psid. to 100 psid.)

Function - To measure the drop in pressure across the test section

9.1.4 Alarm Circuits

In order to prevent inadvertent burnout of the test section the loop is provided with various alarm circuits. The following four loop conditions are annunciated as light alarms on the instrument panel:

1. High temperature on the surface of the test section.
2. High temperature of the heat exchanger coolant water at outlet of heat exchanger.
3. High pressure at accumulator.
4. Low pressure at accumulator.

"Push to test" lights provide a means of checking the operating of the four lamps.

The test section is protected from burnout by the tripping of CB-1 under the following conditions:

1. Pump failure due to low pump cooling water flow or high stator temperature.
2. Excessive test section wall temperature. The high limit is set manually by the operator and once tripped will continue to prevent operation until the temperature has fallen below the alarm value and the release button on instrument TIA-2 is pushed.

In case of high pressure excursions there is a safety pressure relief valve set at 2200 psig and a metal rupture disc designed to rupture at 2300 psig. The exhaust from these devices passes through a diffuser and into the drainage system of Ward Hall. The maximum possible temperature of this exhaust is below 212^{o}F in all but extreme cases.

9.1.5 Detail of Test Section

The test section of this loop is a specially instrumented, circular tube, designed to show the phenomena of light water heat transfer. The specifications are summarized below:

Material - Type 316 stainless steel, ASTM Spec. SA213

Size - I.D. 0.250" ± .001"; O.D. 0.500" ± .001"

Length - 5' 3 1/16" ± 1/32"

Heated Length - 4'

There are 25 thermocouples spot-welded to the outer wall of the tube and two pressure taps to measure the pressure drop across the tube. The test section is enclosed in a protective shroud and is insulated, disposed vertically, and has flow directed upwards in the forced convection mode. As shown in Fig. 12 the inner space between the test section and the shroud contains the thermocouple wires. The section itself is mounted between springs to allow for expansion due to heat generated by the voltage impressed across the test section. Figure 12 shows the test section with insulation and half of the steel shroud removed exposing the arrangement of the thermocouples. They are equally spaced along the heated length.

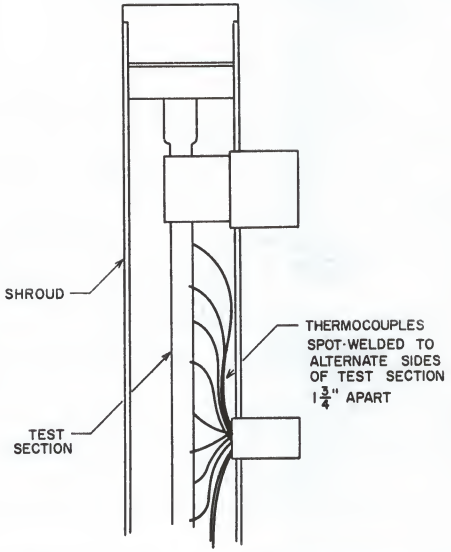

FIGURE 12: DETAIL OF TEST SECTION SHOWING CR - AL THERMOCOUPLES

9.1.6 Operation

The following steps are necessary in order to perform the indicated operation

9.1.6.1 Filling From A Dry Condition At Zero Pressure

Reference to Fig. 9

1. The main or tap water supply valves V-24, V-27, and V-28 are closed.
2. Open all remaining valves in loop system with the exception of V-22.
3. Close bleed valve V-14 on accumulator branch and pressurize accumulator such that the diaphram will occupy about half the volume of the accumulator when the static water pressure is applied. There is a low range nitrogen regulator available which can be used for this purpose. The required pressure is between 10 and 16 psia. This should allow sufficient expansion of loop contents at the highest pressure.
4. Open teflon valve connecting loop to distilled water tank. Open V-22 gradually to allow water to flow into the loop, and close V-23 when water starts to flow from this valve. Valve - 30 and V-29 may be closed at this point.
5. Close all vent and drain valves when water flows from them. The anticipated sequence is V-12, V-32, and V-31.
6. Continue filling loop with water until flow from the main vent, i.e., at valve V-19, and continue until all air has been removed from the system. Valve 23 should be opened briefly to allow the

passage between V-23 and V-8 to fill.

7. Close valve V-19.
8. Close V-22 after 5 minutes.
9. Close teflon valve to still.
10. Isolate deionizer circuit by closing valves V-21, V-8, V-30 and V-6.

9.1.6.2 Start-up Procedure

1. Check the following valves closed:

   Filling circuit: V-24, V-21, V-22.

   Deionizer circuit: V-7, V-30, V-29.

   Hydrazine circuit: V-23, V-31, V-8

   Pump by-pass: V-6.

   Accumulator: V-32, V-14.

   Vent and drain: V-12, V-19.

2. Check main loop valves open: V-1, V-2, V-3, V-4, V-5.
3. Check accumulator line V-34 open.
4. Set the manual power control on the control panel to the minimum setting, and close the wire screen transformer door. (Electrical interlocks prevent CB-1 from being closed unless the above conditions are satisfied.) Close circuit breaker CB-2.
5. Open V-28 on pump cooling line until relay clicks indicating safe flow conditions. Adjust to the desired rate by FC-3.
6. Open valve V-27 for heat exchanger cooling water. Adjust to desired value of FI-2.
7. Start pump at switch on instrument panel.

9.1.7 Additional Information

There are also available systems for deionizing the water in the loop and a method to remove the free oxygen in the water. Since distilled water is used to fill the loop, these treatments were deemed unnecessary and are not included in this appendix. Manuals exist containing more information on operation and maintenance for the loop and its associated equipment. (4, 5) Working drawings of the test section and schematic drawings of electrical networks in detail can be found in the Heat Transfer Loop File, Department of Nuclear Engineering, Kansas State University.

9.2 APPENDIX B: AN EXPERIMENT IN BASIC HEAT TRANSFER

9.2.1 Introduction

The following experiment was adapted from similar experiments performed at Argonne National Laboratory (11,14), and was designed with the aim of providing basic, as well as specific data for water in the forced convection mode of heat transfer as well as for frictional pressure drop. The experiment is designed also to show the effect of flow rate and pressure on heat transfer coefficients as well as to compare the results with established and proposed correlations. The experiment was performed at Kansas State University under the auspices of the Nuclear Engineering Department as part of the program of a course entitled Nuclear Reactor Technology II Laboratory.

9.2.2 Theory*

The analytical expression for the transfer of heat by convection involves a quantity called the film coefficient or the heat transfer coefficient. The equation for convection heat transfer is written as

$$q = h A \Delta T_f , \qquad \text{(B-1)}$$

or the heat flow in Btu/hr is equal to some proportionality factor times heat transfer area, times some temperature differential between the surface and the fluid, where h is a function of fluid properties, geometry, and velocity. If one divides the above equation by A, one has a point occurrence where q/A

---

* The nomenclature used in this section is that of Knudsen and Katz, Fluid Dynamics and Heat Transfer, McGraw Hill Co., New York, 1958.

is the heat flux at some point. And if one knows the fluid temperature, heat flux and coefficient of heat transfer, one may calculate ΔT_f and predict the surface temperature at a given point from the relation

$$t_{surface} = t_{fluid} + \Delta T_f \qquad (B-2)$$

Thus it can be seen that a method of predicting h is valuable in today's applications of heat transfer principles.

9.2.2.1 Correlations

The analysis of turbulent flow in tubes does not lend itself well to purely theoretical manipulation, particularly the calculation of a heat transfer coefficient. Two of the most popular ways of correlating data have been by dimensional analysis and mass to heat transfer analogies.

Dimensional analysis is merely the formation of dimensionless groups by looking at the continuity of the pertinent properties and variables. For example if h is assumed to be a function of the various properties of water in motion in a tube:

$$h = f\ (\rho,\ u,\ \mu,\ D,\ C_p,\ k) \quad \{Q/tL^2\tau\} \qquad (B-3)$$

where the units of "h" are $Btu/ft^2\text{-}hr\text{-}^oF$. Examining the units of all the variables and setting their product equal to the units of h with each property raised to an exponent as yet unknown as below, produces

$$\frac{Q}{tL^2\tau} = \left(\frac{M}{L^3}\right)^a \left(\frac{L}{\tau}\right)^b \left(\frac{M}{L\tau}\right)^c \left(L\right)^d \left(\frac{Q}{Mt}\right)^e \left(\frac{Q}{tL\tau}\right)^f \qquad (B-4)$$

Equating the coefficients of each variable one has four equations in six unknowns, and solving the system in terms of e and b produces

$$\begin{aligned} f &= 1 - e \\ c &= e - b \\ a &= b \\ d &= b - 1 \end{aligned} \tag{B-5}$$

and collecting the properties into dimensionless groups one arrives at the familiar Dittus-Boelter equation

$$hD/k = c\left(\frac{\rho\ u\ D}{\mu}\right)^{b} \left(\frac{\mu\ C_p}{k}\right)^{e} \tag{B-6}$$

where c, b, and e are determined by evaluating experimental data. Colburn (6) found these constants to be c = 0.023, b = 0.8, e = 0.333. This formula was proposed in 1933 and is widely used today for forced convection heat transfer coefficients.

The second method used to correlate data is the analogy. An analogy is a relationship or similarity between the equation describing two systems; in this case between heat transfer and fluid friction; i.e., the movement of heat between a surface and a fluid follows the same laws as the movement of momentum between the surface and the fluid.

For flow in a tube the frictional loss from fluid mechanical considerations is

$$-\frac{d\ P_f}{dz} = 2f\ \frac{\rho\ \overline{U}^2}{g_c\ D} \quad \text{where } \overline{U} \text{ is the average velocity.} \tag{B-7}$$

If the mass flow rate is m, Eq. (B-7) can be written

$$-\frac{\pi D^2}{4}\ g_c\ \frac{d\ P_f}{dz} = \frac{\pi D^2}{4m}\ \frac{2f\ \overline{U}\ \rho\ m\ \overline{U}}{D} \tag{B-8}$$

The left hand term is the rate of momentum transfer/ft. and $m\overline{U}$ is the momentum of the fluid with respect to the wall. Reynolds' analogy states that

$m C_p \frac{d T_b}{dz}$ may be substituted for the left side of Eq. (B-8) and $m C_p (T_w - T_b)$ for $m \bar{U}$ where $m C_p \frac{d T_b}{dz}$ is the rate of heat transfer/ft. and the latter term is the sensible heat in relation to the wall.

$$m C_p \frac{d T_b}{dz} = \frac{\pi D^2}{4m} \frac{2f \bar{U} \rho}{D} m C_p (T_w - T_b) \qquad \text{(B-9)}$$

Remembering that $m = \rho A \bar{U} = \frac{\pi D^2}{4} \rho \bar{U}$ one arrives at an expression for the change in bulk temperature with respect to z

$$\frac{d T_b}{dz} = \frac{2f}{D} (T_w - T_b) \qquad \text{(B-10)}$$

Now taking a heat balance on a differential fluid volume results in

$$\frac{\pi D^2}{4} \bar{U} C_p \rho \, d T_b = h \pi D (T_w - T_b) \, dz \qquad \text{(B-11)}$$

where the term on the right represents the heat transferred to the fluid and the term on the left represents its resultant temperature rise. Using Eq. (B-10) one can derive a simple formula for h

$$h = \frac{f}{2} \bar{U} C_p \rho \qquad \text{(B-12)}$$

and rearranging this to arrive at some familiar groupings and the final expression

$$\frac{hD}{k} = \frac{f}{2} \left(\frac{\bar{U} D \rho}{\mu} \right) \left(\frac{\mu C_p}{k} \right) \qquad \text{(B-13)}$$

The Reynolds' analogy did not take into account the velocity distribution near the wall and in the core, using as he did the average velocity of the fluid in the tube. Prandtl attempted to correct that by assuming a laminar sub-layer near the wall with a linear velocity distribution, and by assuming a turbulent core. The equations describing turbulent flow are as follows:

$$\frac{\tau g_c}{\rho} = (\nu + \varepsilon_m) \frac{du}{dy} \tag{B-14}$$

$$\frac{q_r}{A_r C_p \rho} = -(\alpha + \varepsilon_H) \frac{dT}{dy} \tag{B-15}$$

where $\nu = \frac{\mu}{\rho}$ and $\alpha = \frac{k}{\rho C_p}$. The epsilons are characteristics of turbulent flow and are a measure of the amount of mixing taking place. They are a function of the time weighted average of the product of the instantaneous velocities. In the laminar sub-layer they are zero because all flow is streamlined and no mixing takes place between layers. If one integrates from y = 0 to y = δ_1, the thickness of the laminar sub-layer remembering at y = 0, $\tau = \tau_w$ and $\frac{q_r}{A_r} = \frac{q_w}{A_w}$, expressions for the velocity and temperature drop at y = δ_1 are derived.

$$U_{\delta_1} = \frac{\tau_w g_c \delta_1}{\rho \nu} \text{ and } T_w - T_{\delta_1} = \frac{q_w \delta_1}{A_w C_p \rho \alpha} \tag{B-16}$$

Eliminating δ_1 one finds

$$\frac{U_{\delta_1} \rho \nu}{\tau_w g_c \alpha} = \frac{A_w C_p \rho}{q_w} (T_w - T_{\delta_1}). \tag{B-17}$$

For the turbulent core, Reynolds' analogy is used to express h. The factor f/2 is eliminated by utilizing the definition of a velocity known as the friction velocity:

$$u^* = \bar{U} \sqrt{f/2}; \; f/2 = \frac{u^{*2}}{\bar{U}^2} = \frac{\tau_w g_c}{\rho \bar{U}^2}; \; h = f/2 \; \bar{U} C_p \rho = \frac{\tau_w g_c}{\rho \bar{U}} C_p .$$

Using this value of h in an equation for q_w we get

$$h A_w (T_w - T_b) = q_w; \; \frac{C_p \rho (T_w - T_b)}{q_w / A_w} = \frac{\bar{U}}{\tau_w g_c / \rho} . \tag{B-18}$$

Subtracting Eq. (B-17) from Eq. (B-18) where $\frac{\nu}{\alpha} = Pr = 1$

$$\frac{\{\overline{U} - U_{\delta_1} (\frac{\nu}{\alpha})\}\rho}{\tau_w g_c} = \frac{A_w C_p \rho}{q_w} (T_{\delta_1} - T_b) \tag{B-19}$$

Adding Eq. (B-19) to Eq. (B-17)

$$\{\overline{U} + U_{\delta_1} (\frac{\nu}{\alpha} - 1)\} \frac{\rho}{\tau_w g_c} = \frac{A_w C_p \rho}{q_w} (T_{\delta_1} - T_b) \tag{B-20}$$

Using the definitions of f and h and rearranging

$$\frac{\{\overline{U} + U_{\delta_1} (Pr - 1)\}}{\overline{U}^2 (f/2)} = \frac{C_p \rho}{h} \tag{B-21}$$

From the universal velocity distribution $\frac{U_{\delta_1}}{\overline{U}} = 5 \sqrt{f/2}$ and we arrive at the Prandtl analogy.

$$\frac{h D}{k} = \frac{Pr\ Re\ (f/2)}{1 + 5 \sqrt{f/2}(Pr - 1)} \tag{B-22}$$

Von Karmann utilized the universal velocity profile to derive his analogy, similar to the Prandtl and Reynolds and of the form

$$\frac{h D}{k} = \frac{f/2\ Re\ Pr}{1 + 5 \sqrt{f/2}\,[Pr - 1 + \ln\{1 + 5/6\ (Pr - 1)\}]} \tag{B-23}$$

The analogy which one would expect to be the most accurate is Martinelli's. The conditions in the loop closely approximate those used in his assumptions. These conditions are

(1). Velocity and temperature profiles are fully developed. Entrance effects are neglected.

(2) The fluid properties are independent of temperature.

(3). There is a uniform heat flux along the wall.

The shear at any point y (measured from r_w) is related to the shear at the wall by

$$\tau = \left(1 - \frac{y}{r_w}\right)\tau_w \tag{B-24}$$

Martinelli assumes the same linear distribution for the rate of heat transfer across the tube as for the shear.

$$\frac{q_r}{C_p \rho A_r} = \frac{q_w}{C_p \rho A_w}\left(1 - \frac{y}{r_w}\right). \tag{B-25}$$

The equations for turbulent flow become

$$\frac{\tau_w g_c}{\rho}\left(1 - \frac{y}{r_w}\right) = (\nu + \epsilon_m)\frac{du}{dy} \tag{B-26}$$

$$\frac{q_w}{\rho C_p A_w}\left(1 - \frac{y}{r_w}\right) = -(\alpha + \epsilon_H)\frac{dT}{dy} \tag{B-27}$$

The Nusselt number (Nu) is defined as

$$Nu = \frac{h D}{k} = \frac{-D}{T_w - T_b}\left(\frac{\partial T}{\partial y}\right)\Bigg|_{y = 0} \tag{B-28}$$

The quantity ϵ_H is assumed proportional to ϵ_m; ϵ_m is solved for using the universal velocity profile, ϵ_H is then solved for in terms of ϵ_m and the second equation is integrated. The results after some manipulations is the Martinelli analogy

$$Nu = \frac{\frac{\epsilon_H}{\epsilon_m}\sqrt{f/2}\left(\frac{T_w - T_c}{T_w - T_b}\right) \quad Re\ Pr}{5\left\{\frac{\epsilon_H}{\epsilon_m} Pr + \ln\left(1 + 5\frac{\epsilon_H}{\epsilon_m} Pr\right) + 0.5\, F_1 \ln\frac{Re}{60}\sqrt{f/2}\right\}} \tag{B-29}$$

The factors $(T_w - T_c)/(T_w - T_b)$ and F_1 are constants whose values vary with Re and Pr. They are tabulated for some values of Re and Pr in Table V and VI.

9.2.2.2 Universal Velocity Distribution

Since this distribution is used in two of the above analogies, some information concerning it is in order. Fluid in a pipe does not flow at the same speed due to friction between the wall and fluid and between the water molecules themselves. For convenience the inner area of the pipe is divided into three sections according to the type of flow believed to exist in each region. Closest to the wall is the laminar sublayer, where flow is parallel or streamlined. At the center is a turbulent core where a mixing action takes place and between the two is the buffer layer which combines characteristics of each.

If u* is the friction velocity defined as $\sqrt{\frac{\tau_w g_c}{\rho}}$, then in the laminar sub-layer $\left.\frac{du}{dy}\right|_{y = \delta_1} = \frac{U_{\delta_1}}{\delta_1}$, i.e., a linear distribution is assumed. Utilizing the definition for shear; $g_c \tau_w = \mu \left.\frac{du}{dy}\right|_{y = 0} = \mu \frac{U_{\delta_1}}{\delta_1}$. Taking the Prandtl velocity distribution

$$\frac{u}{u^*} = \frac{u_{max}}{u^*} + 2.5 \ln \frac{y}{r_w} \tag{B-30}$$

and substituting $y = \delta_1$, Eq. (B-21) becomes

$$\frac{U_{\delta_1}}{u^*} = \frac{u_{max}}{u^*} - 2.5 \ln \left(\frac{r_w u^*}{\frac{U_{\delta_1}}{u^*} \nu} \right) \tag{B-31}$$

Collecting constants $\left(\frac{U_{\delta_1}}{u^*} \right)$

Table V. Values of F_1 for Martinelli's analogy.

Pe / Re	10^4	10^5	10^6
10^2	0.18	0.098	0.052
10^3	0.65	0.45	0.24
10^4	0.92	0.83	0.65
10^5	0.99	0.985	0.980
10^6	1.00	1.00	1.00

Table VI. Values of $(T_w - T_b)/(T_w - T_c)$ for Martinelli's analogy.

Pr / Re	10^4	10^5	10^6	10^7
10^{-1}	0.692	0.761	0.823	0.864
1.0	0.865	0.877	0.897	0.912
10	0.958	0.962	0.963	0.966

$$\frac{u_{max}}{u^*} = C' + 2.5 \ln \frac{r_w u^*}{\nu} \tag{B-32}$$

and substituting Eq. (B-22) in Eq. (B-21)

$$\frac{u}{u^*} = C_1 + 2.5 \ln \frac{y u^*}{\nu} \text{ or } u^+ = C_1 + 2.5 \ln y^+ \tag{B-33}$$

It has been found by experiment that in the laminar sublayer ($y^+<5$)

$$u^+ = y^+ \tag{B-34}$$

in the buffer layer ($5<y^+<30$)

$$u^+ = -3.05 + 5.0 \ln y^+ \tag{B-35}$$

and in the turbulent core ($y^+<30$) $u^+ = 5.5 + 2.5 \ln y^+$ (B-36)

There are disadvantages to this involving continuity at $y = r_w$ and improvements have been made so that this distribution is the one most acceptable.

9.2.2.3 Other Calculations

Other parameters are measured in this experiment including frictional pressure drop and inlet and outlet bulk temperature. The equation used to check the change in bulk temperature and which was found to be one of the more accurate predictions is derived from a heat balance on an element of fluid dz in length, in a time interval dτ

$$\frac{d T_b}{dz} = \frac{\pi D q''}{\omega C_p} \tag{B-37}$$

One can also use this equation to derive an equation for h

$$\frac{\omega C_p}{\pi D} \frac{d T_b}{dz} = q'' = h (T_w - T_b) \tag{B-38}$$

$$h \, dz = \frac{d T_b}{T_w - T_b} \frac{\omega C_p}{\pi D} \tag{B-39}$$

Another equation of importance is that for the temperature drop through the wall. (11)

$$\Delta t_w = - \frac{r_1 q''}{24(r_o^2 - r_i^2)k} \left\{(r_o^2 - r_i^2) - 2r_o^2 \ln \frac{r_o}{r_i}\right\} * \qquad (B\text{-}40)$$

9.2.3 Experiment Performance

9.2.3.1 Procedure

1. Start cooling water through the pump by means of V-28. Open valve until FC-3 = 2.5.

2. Start cooling water through the heat exchanger by V-27 until FI-2 = 70%.

3. Adjust accumulator to desired pressure. To lower the pressure, open V-14 and allow some nitrogen to escape. To raise the pressure close V-14 and open V-15 if it is not open. Close the load valve on the regulator, open the bleed valve. Open the load valve slowly and adjust to the desired pressure.

4. Turn on the pump by switch on the control panel and adjust the flow rate in the loop by V-1 reading FI-1.

5. Turn valve on the compressor to admit air to the differential pressure transmitter. The compressor is on the south wall of the reactor bay.

6. Check experimental values of flux and flow rate with table and graphs of critical flux in the operation and maintenance manual (4). Make

* r in inches

sure the safety limits are not exceeded.

7. Turn variac to minimum position, check transformer enclosure door closed and close CB-1, on back of the transformer complex.

8. Adjust variac slowly to experimental value of heat flux, using the wattmeter on the control panel, and its accompanying chart.

9. Read FI-2, FI-1, FC-3, W-1 while keeping all parameters constant.

10. Read

TI-3	Test Section Temperature
TI-1	Test Section Inlet Coolant Temperature
TI-8	Test Section Outlet Coolant Temperature
TI-7	Pump Inlet Coolant Temperature
PI-6	Test Section Pressure Drop
TIA-2	Test Section Temperature Alarm
PI-1,PI-2	Loop Pressure
PIA-3	Accumulator
V-1	Voltage Across Test Section
A-1	Current Through Test Section

11. Return to 3. and repeat.

9.2.3.2 Calculations to be Performed For Each Condition

1. Plot test section temperatures and water temperature assuming a straight line distribution.

2. Calculate dT_b from graph and equation and compare.

3. Calculate an average $T_w - T_b$ from the graph after correcting for the temperature drop through the wall.

4. Using an average T_b calculate the Reynolds number and h by the Dittus-Boelter equation.

5. Calculate h by $h = \frac{q}{A} \frac{(T_w - T_b)}{T_w - T_b}$

6. Calculate h by $h = \frac{1}{z} \frac{(T_{bo} - T_{bx})}{(T_w - T_b)} \frac{\omega C_p}{\pi D}$

7. Calculate h by Reynolds, Prandtl, Von Karmann, and Martinelli analogies.

8. Make a table displaying the results of the heat transfer coefficient calculations.

9. Calculate the frictional pressure drop and compare it with the measured value.

9.2.3.3 Discussion

1. What assumptions are made in each calculation of h? (See e.g. Knudsen and Katz, Fluid Dynamics and Heat Transfer.)

3. Find an empirical correlation for h which describes the loop behavior better than the analogies above. This may be found in another reference rather than original.

9.2.3.4 Prescribed Runs

The parameters at which the runs are made are indicated in Table VII below.

Table VII. Parameters of the experimental runs.

Run	1	2	3	4
Pressure (psia)	1000	1000	1300	1300
Flow rate/Max. flow	1.00	0.70	1.00	0.80
Power (KW)	50.0	50.0	50.0	50.0
Critical Power (KW)	66.0	59.8	50.0	50.0
FC-3 (GPM)	2.40	2.40	2.40	2.40
FI-2 (fractional)	0.70	0.70	0.70	0.70

9.2.4 Instructor's Guide

9.2.4.1 Outline of Lesson Plan

I. One hour or less on function and make-up of loop.

A. Includes equipment discussion.

B. Includes measurement technique.

II. Two hours in performance of experiment.

A. Four runs at one pressure (1000 psi); two each at a given flow rate; first group calculations (1 hr.).

B. Four runs at one pressure (1300 psi); two each at a different flow rate; second group calculations (1 hr.).

III. One hour lecture on the theory of calculations.

A. Includes dimensional and theoretical analysis of the heat transfer coefficient.

B. Includes discussion and derivation of equations used in calculations.

IV. One hour to begin calculations and plotting.

9.2.4.2 Results

The required information to be handed out to the students should include information regarding both theory and procedure. A maximum of 9-10 people can perform this experiment although smaller numbers could be employed. The actual time was found to be about 3-4 hours in practice depending on the organizational ability of various individuals in the groups. Sample data is shown for four runs in Table VIII. A computer program is available to cal-

culate the various quantities called for in the calculations although the responsibility of this experiment make additional calculation unnecessary since the initial calculations have already been made.

Table VIII. Data taken from the four runs performed .

Thermocouple designation	Run 1	Run 2	Run 3	Run 4
TI-1	98°F	90°F	98°F	99°F
TI-7	90	85	91	90
TI-8	183	220	182	209
T 1	616	667	622	649
T 2	588	637	592	620
T 3	606	654	610	636
T 4	581	628	586	611
T 5	592	636	597	620
T 6	576	620	581	604
T 7	572	613	577	598
T 8	580	618	585	604
T 9	564	603	568	589
T 10	572	608	578	596
T 11	549	585	555	573
T 12				
T 13	547	580	553	570
T 14	567	596	570	587
T 15	538	567	533	559
T 16	564	592	569	584
T 17	527	555	533	550
T 18	558	586	563	579
T 19	532	558	535	549
T 20	551	576	555	570
T 21	521	543	523	538
T 22	549	574	553	566
T 23	523	544	526	538
T 24	537	555	539	550
TIA - 2				
Pressure indic.				
Δ PI-6	15.3 psi	6.9 psi	15.6 psi	9.7 psi
PI-1	980	990	1230	1235
PI-2	1090	1090	1320	1320

Table IX. Calculated results of experiment.

	Run I	Run II	Run III	Run IV
Calculated $T_w - T_b$	133	156	139	147
Calculated ΔT_b	84.8	121	84.8	106
Experimental ΔT_b	85.0	123	84.0	112
Reynolds' No.	108,394	85,132	107,964	96,401
Calculated ΔP	15.39	7.59	15.39	9.89
Experimental ΔP	15.4	7.0	15.6	9.7
Heat Transfer Coefficient				
h(Dittus-Boelter)	6,978	5,524	6,964	6,125
$h(\dot{Q}/\Delta T_{w-b})$	4,889	4,214	4,682	4,432
$h(\frac{\Delta T_b * w * C_p}{\pi * D * \Delta T_{w-b}})$	4,896	4,370	4,633	4,686
h(Reynolds)	12,373	8,683	12,372	9,909
h(Prandtl)	8,542	6,337	8,525	7,205
h(Von Karmann)	7,408	5,545	7,391	6,301
h(Martinelli)	6,150	4,650	6,070	5,240

9.3 APPENDIX C: HEAT LOSS FROM THE TEST SECTION

In order to investigate the accuracy or dependability of the experimental data, tests attempting to effectively evaluate the heat losses from the test section were performed. These tests were also designed to check the uniformity of the thermocouple reading, indicative of the wall temperature of the test section. Certain modifications were made in the electrical safety interlock to permit operation of the heating voltage without fluid circulating through the tube and without pump operation. Contacts which would normally open when the above conditions are realized are bypassed as illustrated in Fig. 13.

The geometry of the test section is shown in Fig. 14. The surrounding insulation is not in one piece but in some parts consists of irregular sections forming in actuality a tight, inch thick coating on the shroud surrounded by a larger, looser fitting shell of one inch or thicker.

When a small voltage is applied to the test section it will rise in temperature until the heat losses are equal to the heat generated in the section. Due to the length of time it was found to require for the test section to reach equilibrium, an alternate approach was used in conjunction with it.

From geometry considerations it was apparent that the significant losses would be by convection to the air surrounding the tube and by radiation to the shroud. It was noted that after the test section reached a final temperature of approximately 800°F, its temperature decreased at the rate of less than 1°/sec. The heat loss in Btu/hr can be expressed as follows:

$$q_L = h \Delta T_a \, dA \quad \text{and} \quad q_L = \rho C_p \, dv \frac{dT}{d\tau}$$

Solving for h produces

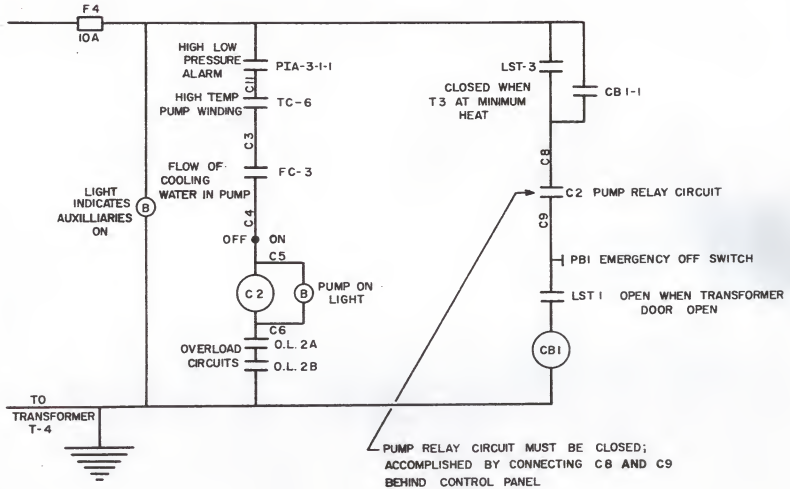

FIGURE 13: SCHEMATIC OF ALARM CIRCUIT

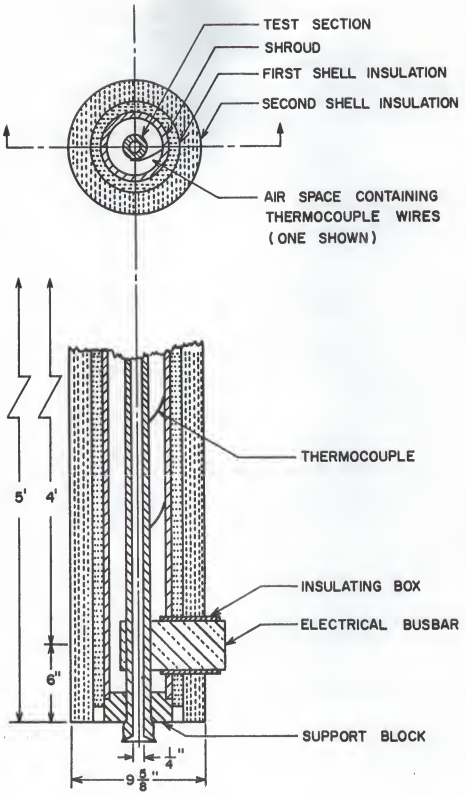

FIGURE 14: TEST SECTION DETAIL

$$h = \rho C_p \frac{dT}{d\tau} \frac{dv}{dA} \frac{1}{\Delta T_a} \text{ where } \frac{dv}{dA} = \frac{(r_o^2 - r_i^2)}{2(r_o + r_i)} \qquad (C\text{-}1)$$

If it is assumed that the heat lost in raising the air temperature in the inner column is negligible, the denominator becomes $2\Delta T_a r_o$ and

$$h = \frac{.470}{\Delta T_a} \frac{dT}{d\tau} \qquad (C\text{-}2)$$

The heat transfer coefficients were generally found to be less than 10 Btu/hr-ft $-^oF$ with the thermocouples nearer the end generally found to have the higher coefficients, as would be expected from the measured temperatures of the test section at these points.

Since heat flux is directly proportional to this coefficient some idea of the heat loss in relation to the operating heat flux may be obtained by examining the ratio to the two coefficients. An experiment has shown the magnitude of the operating heat transfer coefficient to be approximately 5×10^3 Btu/hr-ft $-^oF$, resulting in an error of less than .5%. As operating time increases the temperature of the surrounding air will increase, decreasing the heat loss and reducing this error even more.

Typical values of these computed heat transfer coefficients are tabulated in Table X. The temperature of the air at the midpoint of the loop was measured approximately by TC-12 which is no longer welded to the test section, and the temperature was found to vary according to how long the voltage was applied to heat the test section. In the experiment each thermocouple on the test section was heated to 500^oF; then the power was shut off and the test section was allowed to cool. The temperature indicated by the thermocouple was recorded every 30 seconds. For the calculations of h the temperature difference has been assumed to be equal to approximately 300^oF.

Table X. Sample values of film coefficient and experimental data.

# Thermocouple	Temperature at 0 sec. ^{o}F	Temperature 30 sec. ^{o}F	Temperature 90 sec. ^{o}F	h_{90}* Btu/hr-ft^2-^{o}F	h_{30}*
1	500^{o}F	455^{o}F	270^{o}F	14.75	8.45
2	-	481	448	3.25	3.57
3	-	484	456	2.75	3.01
4	-	485	460	2.51	2.82
7	-	485	458	2.63	2.82
9	-	487	460	2.51	2.44
11	-	486	459	2.57	2.63
13	-	484	457	2.70	3.01
17	-	485	454	2.89	2.82
21	-	478	438	3.89	4.14
22	-	474	430	4.39	4.89
23	-	466	409	5.70	6.49
24	-	434	340	10.0	12.4

* h_{90} was computed for a time interval of 90 seconds, h_{30} for a time interval of 30 seconds.

The h's can be used in conjunction with the measured wall temperatures to predict the temperature of the air surrounding the test section. The results of this calculation are shown in Fig. 15. The distribution is not a surprising one in that air temperature is expected to vary with height and decrease at the ends where there are better properties of circulation. The shroud and surrounding insulation is not airtight which provides some air circulation. The insulation is not of one piece but is sectioned, consisting of an inner and outer shell and divided in the middle which may account for the sharp drop in air temperature at the center. Fortunately it has been shown that the heat losses are less than 0.5% of generated power and the erratic coefficients are not a factor during operation. The coefficients calculated over the 90 second interval are more uniform than those calculated over the 30 second interval. Further extension of the interval would not

likely change the accuracy due to the change in slope of T_w versus (time). This behavior is shown in Fig. 16. A similar treatment for ramp changes in power generation is available in (13).

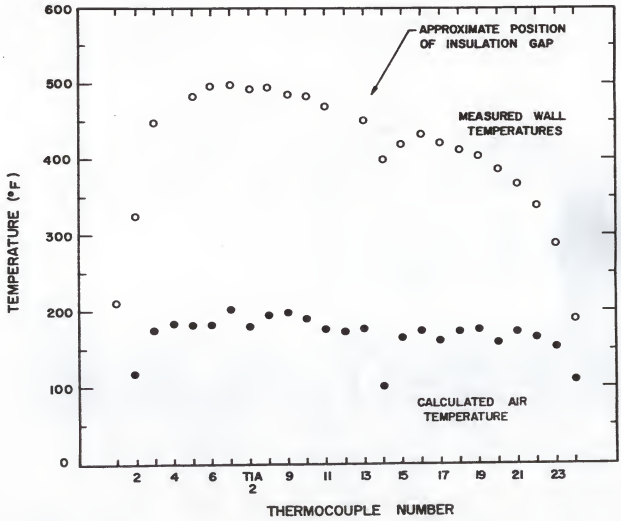

FIGURE 15 : WALL TEMPERATURE OF TEST SECTION AND TEMPERATURE OF SURROUNDING AIR.

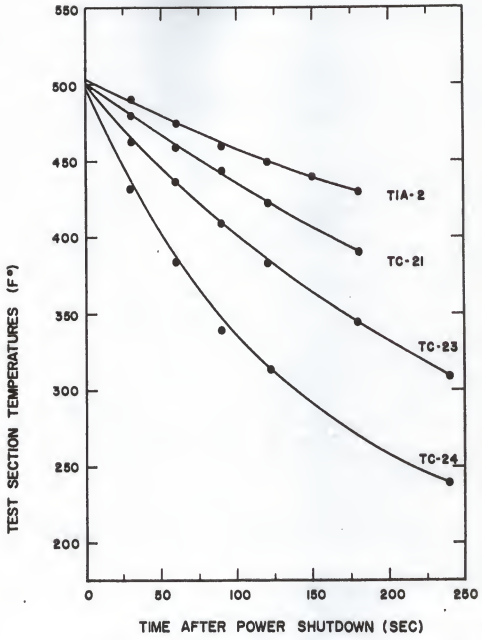

FIGURE 16: WALL TEMPERATURE BEHAVIOR AFTER POWER-SHUTDOWN

A VELOCITY TRANSFER FUNCTION ANALYSIS OF FORCED CONVECTION HEAT TRANSFER

by

MICHAEL KENT MAHAFFEY

B. S., Kansas State University, 1964

AN ABSTRACT OF
A MASTER'S THESIS

submitted in partial fulfillment of the

requirements for the degree

MASTER OF SCIENCE

Department of Nuclear Engineering

KANSAS STATE UNIVERSITY
Manhattan, Kansas

1966

ABSTRACT

This study describes a perturbation technique for obtaining the outlet coolant temperature - velocity transfer function for a circular stainless steel tube. A computer program is used to evaluate the real and imaginary components of this transfer function for various values of frequency and various initial velocities. After constructing Bode plots using a dimensionless frequency which is inversely proportional to the initial velocity, the transfer function is approximated by a series of lead or lag terms which are linear functions of the initial velocity; thus resulting in a simple, easily calculated transfer function for engineering applications. This approximated transfer function is used to predict the response of the outlet coolant temperature to a step change in velocity. Predicted responses are compared with experimental data obtained from the pressurized water heat transfer loop operated by the Nuclear Engineering Department of Kansas State University.

The results of this comparison showed a correlation to within ± 4°F between predicted and experimental values of the final temperature caused by a known perturbation of the velocity. Also the shape of the theoretical response curve followed that of the experimental response curve closely when the former was corrected for thermocouple response. Generally the best results were produced when an exact solution was made for the final temperature and the transient response predicted from the perturbation technique. The largest errors in final temperature occured at low initial velocity due to the relative magnitude of the step change and the inapplicability of the perturbation theory.

The appendices of this thesis contain material relating to the apparatus utilized in this experiment along with a section regarding heat losses from the test section. Also included is a laboratory experiment currently being performed as part of the course of study in Nuclear Reactor Technology II Laboratory which was evolved during the course of this study.